UCRL 8387

UNIVERSITY OF CALIFORNIA

Radiation Laboratory

I. A METHOD FOR DETERMINING RADIATIVE LIFETIMES OF HIGH-TEMPERATURE MOLECULES
II. THE PROBABILITY OF SPONTANEOUS NUCLEAR REACTION IN MOLECULAR HYDROGEN

BERKELEY, CALIFORNIA

DISCLAIMER

This document was prepared as an account of work sponsored by the United States Government. While this document is believed to contain correct information, neither the United States Government nor any agency thereof, nor the Regents of the University of California, nor any of their employees, makes any warranty, express or implied, or assumes any legal responsibility for the accuracy, completeness, or usefulness of any information, apparatus, product, or process disclosed, or represents that its use would not infringe privately owned rights. Reference herein to any specific commercial product, process, or service by its trade name, trademark, manufacturer, or otherwise, does not necessarily constitute or imply its endorsement, recommendation, or favoring by the United States Government or any agency thereof, or the Regents of the University of California. The views and opinions of authors expressed herein do not necessarily state or reflect those of the United States Government or any agency thereof or the Regents of the University of California.

UCRL-8387
Chemistry-General

UNIVERSITY OF CALIFORNIA
Radiation Laboratory
Berkeley, California

Contract No. W-7405-eng-48

I. A METHOD FOR DETERMINING RADIATIVE LIFETIMES OF HIGH-TEMPERATURE MOLECULES

II. THE PROBABILITY OF SPONTANEOUS NUCLEAR REACTION IN MOLECULAR HYDROGEN

Richard G. Brewer

(Thesis)

July 21, 1958

Printed for the U. S. Atomic Energy Commission

This report was prepared as an account of Government sponsored work. Neither the United States, nor the Commission, nor any person acting on behalf of the Commission:

A. Makes any warranty or representation, express or implied, with respect to the accuracy, completeness, or usefulness of the information contained in this report, or that the use of any information, apparatus, method, or process disclosed in this report may not infringe privately owned rights; or

B. Assumes any liabilities with respect to the use of, or for damages resulting from the use of any information, apparatus, method, or process disclosed in this report.

As used in the above, "person acting on behalf of the Commission" includes any employee or contractor of the Commission to the extent that such employee or contractor prepares, handles or distributes, or provides access to, any information pursuant to his employment or contract with the Commission.

I. A METHOD FOR DETERMINING RADIATIVE LIFETIMES OF HIGH-TEMPERATURE MOLECULES

II. THE PROBABILITY OF SPONTANEOUS NUCLEAR REACTION IN MOLECULAR HYDROGEN

Contents

Abstracts I and II 3

Part I 5

Introduction. 5

Apparatus 10

Short-Lifetime Apparatus: Light Modulator 12

1. Optics. 16

2. Electronic Circuitry 17

a. Frequency-reduction unit. 19

b. Automatic frequency control 21

c. Light detector and preamplifier. 23

d. Phase shifter and calibration 23

e. Q-multiplier filter 28

f. Phase detector 30

g. Power supplies 30

Problems Associated with the Photomultiplier 33

Sensitivity of the Apparatus 37

The Lifetime of Acridone: A Discussion of Errors . . . 41

Long-Lifetime Apparatus: Light Modulator 43

A. Electronic Circuitry 47

1. Automatic Frequency Control 47

2. Motor Speed Control 51

B. The Fluorescence Lifetime of Iodine Vapor 51

Part II 60

Acknowledgments 68

Appendixes 69

References 71

I. A METHOD FOR DETERMINING RADIATIVE LIFETIMES OF HIGH-TEMPERATURE MOLECULES

II. THE PROBABILITY OF SPONTANEOUS NUCLEAR REACTION IN MOLECULAR HYDROGEN

Richard G. Brewer

Radiation Laboratory
University of California
Berkeley, California

July 21, 1958

ABSTRACT

Part I. An apparatus for determining the radiative lifetimes of gaseous molecules in excited electronic states is described. The design is based on the work of Bailey and the work of Kromann. The method involves measuring the phase angle ϕ between fluorescent and exciting light, which is modulated. Only a single harmonic of the modulated light is utilized, so that we have $\tan \phi = \omega\tau$, where ω is the angular modulation frequency and τ is the lifetime. Lifetimes can be measured in the range 10^{-5} to 10^{-9} sec to an accuracy of 3%.

By a modification in Bailey's optical design, the sensitivity of his apparatus has been increased about 100-fold. With this change, lifetime measurements can be made under conditions in which self-absorption is unimportant.

The absolute sensitivity of the apparatus was found in terms of the minimum brightness temperature of a light source that would be needed to determine the lifetime of the excited state of one of the sodium D lines. This value was 2200° K and corresponded to a light flux of 5×10^{5} photons/sec striking the photomultiplier. Because light sources with brightness temperatures up to 6000° K exist, the apparatus possesses sufficient sensitivity for a number of molecular lifetime determinations.

It is shown that if the geometry of light falling on the photocathode of a photomultiplier is changed during a measurement, serious errors in the lifetime can result. The effect is associated with the

dispersion in transit time of photoelectrons leaving different areas of the photocathode.

The lifetime of the $^3\Pi_u$ (v' = 26) state of molecular iodine has been found to be 4×10^{-7} sec at 21° C in the saturated vapor. Measurements at 0°C indicate that the fluorescence lifetime is shorter, and therefore 4×10^{-7} sec is to be taken as an upper limit.

An important application of lifetime data to the determination of heats of formation in high-temperature molecules is cited. By this technique it should be possible to determine heats of formation with an accuracy of 1%, in contrast with present techniques, which are usually in error by more than 10%.

Part II. The probability for spontaneous nuclear reaction in molecular hydrogen has been calculated by the use of WKB wave functions. The complete shape of the molecular barrier has been derived from spectroscopic data for the hydrogen molecule and from a perturbation calculation of the helium atom. Use of this potential function showed that the probability of penetrating the molecular barrier (for a ground-state molecule) is greater by a factor of about 10^{15} than of penetrating a Coulomb barrier at the same internuclear distance. The half lives for nuclear reaction in the isotopic molecules H^1H^1, H^1H^2, and H^2H^2 are 5×10^{56}, 5×10^{46}, and 1×10^{54} years.

Part I

A METHOD FOR DETERMINING RADIATIVE LIFETIMES OF HIGH-TEMPERATURE MOLECULES

INTRODUCTION

Very few radiative lifetimes are known for gaseous molecules in electronic transition, in spite of their importance. Most of the values that are available for diatomic molecules have been derived from order-of-magnitude quantum-mechanical calculations.[1] For polyatomic molecules the data are even more scarce.[2] The only high-temperature molecules for which measurements exist are C_2,[3] CN,[4] and OH,[5] and these values are uncertain to an order of magnitude in C_2 and CN and probably to more than 20% for OH.[6]

However, knowledge of the radiative lifetime of a high-temperature molecule could be valuable for obtaining accurate thermodynamic data. To illustrate the point, consider a molecule in an excited electronic state with an average lifetime τ. The emission or fluorescence spectra consist of transitions from the excited state to all lower levels. The probability that any one transition will occur in unit time is $A_{m \to n}$, the Einstein coefficient for spontaneous emission. The sum of all the transition probabilities $\Sigma A_{m \to n}$ is the total probability that the molecule will leave the excited state in unit time. Thus $1/\Sigma A_{m \to n}$ is the average time elapsed in the excited state or

$$\tau = 1/\Sigma A_{m \to n} .$$

If the lifetime τ and the relative transition probabilities for fluorescence are known, say from relative intensity measurements, the absolute transition probabilities $A_{m \to n}$ can be found.

In an absorption experiment the practical quantity k_ν is used. It is defined by the equation

$$I/I_0 = e^{-k_\nu x} , \qquad (1)$$

where I/I_0 is the fraction of light transmitted by the gas and is a function of the frequency ν, and x is the optical path length. It can be

shown that when pressure broadening is small and the Doppler width is significantly larger than the natural width of the line, the maximum absorption coefficient[7] of the line is given by

$$k_0 = \frac{2}{\Delta\nu_D}\sqrt{\frac{\ell n 2}{\pi}}\;\frac{\lambda_0^2}{8\pi}\;\frac{g_m}{g_n}\;NA_{m\to n}\ \mathrm{cm}^{-1}, \qquad (2)$$

where $\Delta\nu_D$ is the Doppler width, g_m and g_n are the degeneracy of excited and lower levels, λ_0 is the wave length and N is the number of molecules per cc. Thus, once $A_{m\to n}$ is known, a measurement of the fraction I/I_0 of light transmitted by the gas at the peak intensity will yield the concentration N.

If, for example, the gaseous molecule X_g is in equilibrium at a pressure P with a solid X_s satisfying the equation

$$X_s = X_g,$$

the free energy of formation of the gas will be

$$\Delta F^o = -RT\ell nP = \Delta H^o - T\Delta S^o. \qquad (3)$$

Since the entropies for most simple high-temperature molecules are available with high accuracy from spectroscopic data, it is possible to determine ΔH to the accuracy to which the temperature and pressure are known. At present above 1000° C there is an uncertainty in the working temperature scale itself. In the range 2000 to 3000° C there is about a 1% uncertainty with respect to the thermodynamic temperature scale.[8] Thus, the main error in ΔH will result from errors in P. Differentiating ℓnP in Eq. (3) with respect to ΔH and dividing both sides by ΔH, one obtains

$$(RT/\Delta H)(dP/P) = (d\Delta H)/\Delta H.$$

An estimation of the errors involved in the lifetime measurement, the optical path length x, and the relative transition-probability measurement indicates an uncertainty in P of about 10%. For typical values of $T = 2000^o$ K and $\Delta H = 100$ kcal, a 10% error in P introduces a 0.4% error in ΔH.

For the most part present determinations of ΔH are of the "second-law type," while the above method is a "third-law technique." Second-law methods make use of the van't Hoff equation,

$$\frac{d\ell nK}{dT} = \frac{\Delta H}{RT^2}$$

and require obtaining the equilibrium constant K at a number of temperatures. From the variation of the equilibrium constant with temperature, a heat of formation can be found. Unfortunately, these measurements introduce a large number of temperature-dependent errors which make the ΔH's uncertain to 10% even in the most favorable cases. Since the third-law technique described above is uncertain to about 0.4%, it is evident that a measurement of this type offers a considerable increase in accuracy.

The purpose of the work reported here was to determine the feasibility of accurate radiative lifetime determinations for gaseous molecules. Although a number of methods have been devised, there are relatively few capable of yielding lifetimes in the 10^{-8} sec range to less than 10% error. The more successful techniques are based on measuring the phase angle between exciting light and fluorescent light that is modulated.[9] Light modulation is accomplished by means of either a Kerr cell or an intermittent diffraction grating. Bailey's technique represents an improvement over past methods, since he isolated a single harmonic of the modulated light.[10] He has shown that if the wave form of the modulated light is not sinusoidal, there need not be a simple relation between the phase shift in the peak of the wave-form and the lifetime of the molecule. However, isolation of a single harmonic does yield a simple relationship between phase shift and lifetime; see Appendix I.

However, Bailey's phase shift measurements were made at a frequency of 5 Mc, a region where small stray capacitances can introduce serious calibration errors. Kromann, using a similar method converted the 5-Mc signal to a 2-kc frequency, made phase-shift

measurements at 2 kc,[11] and uncovered a consistent 8% error in Bailey's values. Kromann's lifetimes are reported to an accuracy of ± 0.5%.

Because of the accuracy possible with this technique, an apparatus was constructed which was patterned after the work of Bailey and Kromann. Another advantage of the method is that it is not dependent on a knowledge of the concentration of the gas. Thus, if concentrations and heats of formation are to be determined, a method of this type must be used.

If accurate measurements are to be made, the gas pressure should be sufficiently low so that collisional deactivation and self-absorption do not influence the lifetime measurements appreciably. Plots of $1/\tau$ versus pressure, both from theory and experiment, show that the effective $1/\tau$ is changing most rapidly at low pressure because of self-absorption.[7] Thus, if the absorption at the center of a line is 10%, self-absorption could introduce a 10% error in the lifetime. If several determinations are made as a function of pressure, extrapolation to zero pressure is possible. On the other hand, if the sensitivity of the apparatus allows measurements to be made at less than 10% absorption, the lifetime error is correspondingly less.

To illustrate the magnitude of pressures required to satisfy 10% peak absorption, consider the 5890 Å sodium transition. Equation (2) can be rewritten in terms of an f value,[7]

$$k_0 = \frac{2}{\Delta \nu_D} \sqrt{\frac{\ell n 2}{\pi}} \frac{\pi e^2}{mc} Nf, \qquad (4)$$

with e the charge of an electron and m its mass. The f value is a measure of the transition probability of an atom or molecule normalized with respect to the transition probability for a classical oscillating electron. For the 5890 Å transition f is 0.70. For 10% peak absorption use of Eq. (1) gives $k_0 x = 0.105$. By assuming a temperature, the value of N can be determined from thermodynamic tables and $\Delta \nu_D$ by direct calculation, (see Eq. (7), p. 39). A judicious choice of the

temperature gives a value for k_0 corresponding to a convenient path length x. For sodium, a pressure of 2.6×10^{-10} atmos (109° C) is required to give 10% peak absorption over a path length of 1.8 cm.[12] If the f value is smaller, the path length or the pressure of the gas can be increased proportionately to give 10% absorption. In any event the pressure is quite low, and under these conditions collisional deactivation is unimportant also.

APPARATUS

The essential elements of the apparatus are shown in Fig. 1. Modulated light of the proper spectral frequency excites gaseous molecules into a higher electronic state. The spectral range can be determined by use of a filter placed between the modulator and the gas. The excited molecules fluoresce by undergoing transitions to all lower levels. Some of the fluorescent light passes onto a photomultiplier via a second filter which rejects the exciting light. The fluorescent and exciting light are out of phase with each other with respect to the modulation frequency, and this phase difference is determined by a phase detector. In order to have a point of reference, it is necessary to replace the fluorescent gas by a scattering substance, such as a $BaSO_4$ sol, which does not introduce a phase shift. Finally, the lifetime τ of the molecule in the excited state is related to the phase angle ϕ between the sol and the fluorescer by the relation

$$\tan \phi = \omega \tau \quad ,$$

where ω is the angular modulation frequency. (See Appendix I for derivation.)

The range of lifetimes to be measured determines what modulation frequency is to be used. Measurements of phase shift should be made as close to 45° as possible because then errors in the lifetime are minimum with respect to errors in the phase shift (see Appendix II). This restriction requires that the modulation frequency be chosen so that phase shifts near 45° are obtained. For fully allowed dipole transitions in the visible spectral region, for example, lifetimes are of the order of 10^{-8} sec, and thus a 5-Mc modulation frequency is desirable.

The apparatus is divided into two parts: the short-lifetime apparatus which covers the range 10^{-7} to 10^{-9} sec, and the long-lifetime apparatus, which covers the range 10^{-5} to 10^{-7} sec. Both methods are represented in Fig. 1. As the optical modulation and electronic circuitry are different, each apparatus is discussed separately.

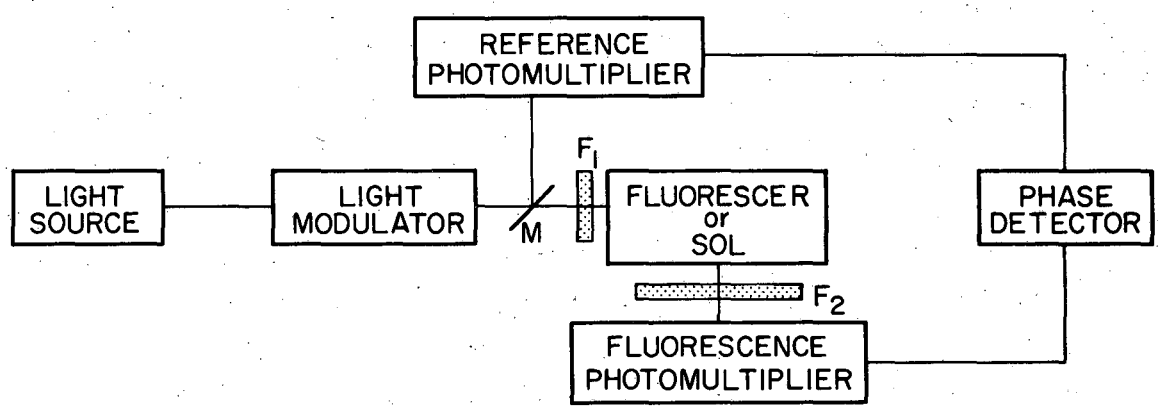

F_1 *Exciting light filter*

F_2 *Fluorescent light filter*

M *Mirror*

MU-15660

Fig. 1. Lifetime apparatus: simplified schematic

Short-Lifetime Apparatus: The Light Modulator

There are relatively few methods for modulating light in the megacycle region. One of these is the Kerr cell, which has the disadvantage of a low optical speed, a low percent modulation of light, and an eventual deterioration of the birefringent liquid on exposure to high electric fields and ultraviolet light. An ingenious method with none of the above disadvantages is based on an invention by Debye and Sears[13] and also independently by Biquard and Lucas.[14] The modulator used in this work follows their design. The modulator consists of an ultrasonic tank filled with water and contains a quartz crystal at one end and a reflecting stainless steel plate at the other. The crystal is driven at its resonant frequency, and by proper positioning of the plate the reflected wave is made to coincide with the incident wave. The resulting standing wave sets up regions of condensation and rarefaction in the liquid whose indices of refraction are changing periodically with time. By passing parallel light through the liquid perpendicular to the direction of propagation of the ultrasonic wave, the light can be periodically dispersed as in a transmission grating (see Fig. 2). The image pattern of the grating consists of a central image, the zero order, and of higher orders on each side. Use of a slit to cut out the higher orders but to allow passage of the zero order results in a modulated light source whose frequency is twice that of the crystal.

The transducer used in the tank was a 1-inch-diameter X-cut quartz crystal obtained from the James K. Knight Co., Sandwich, Ill. Quartz is particularly desirable because it is readily available, cheap, and rugged. An X-cut crystal is used because a compressional thickness vibration is required. Circular-cut crystals have the advantage of being able to stand higher voltages without fracture and of giving more uniform radiation over their surfaces. For an excellent review and list of references in ultrasonics see Cady's book "Piezoelectricity".[15]

In the initial stages of this work, the 1-inch-diameter crystal was mounted over a 15/16-inch-diameter hole in a polystyrene disc.

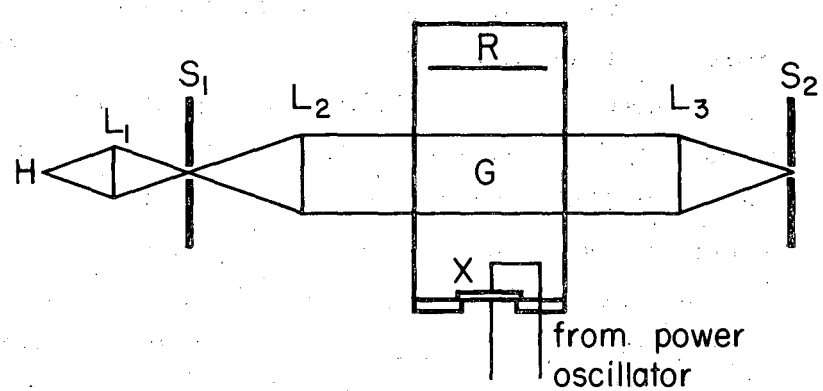

H	*A-H4 Mercury light source*
L_1	*Glass lens, 10 cm focal length, 5 cm diameter*
L_2, L_3	*Glass lenses, 20 cm focal length, 11 cm diam.*
S_1, S_2	*Slits*
X	*X-cut quartz crystal*
R	*Stainless steel reflector*
G	*Ultrasonic standing wave*

MU-15661

Fig. 2. Light-modulating unit (schematic diagram)

The crystal was cemented to the disc by moistening the 1/16-inch overlap with benzene. The disc was in turn cemented to a partition at one end of the ultrasonic tank. The air-side electrode consisted of 15/16-inch-diameter copper foil, 1 mil thick, which was cemented onto the side of the crystal facing into the hole of the disc; electrical contact was made by means of a spring passing through a hole in the partition and pressing up against the foil.

Considerable difficulty was encountered in obtaining a permanent electrode on the water side of the crystal, however. Although sputtering of silver, platinum, or gold is often reported to give stable electrodes, this technique was not available. Instead, vacuum deposition of silver with and without silver plating was tried; electrical contact was made through a fine wire imbedded in a flattened drop of solder which was partly cemented to the electrode. These attempts were generally unsuccessful because of the metal's poor adhesion to quartz. Copper foil cemented onto the face with benzene and polystyrene or Duco cement showed deterioration at the edge because of cavitation. Finally, a satisfactory mounting was obtained by cementing copper foil on both sides of the crystal, but deterioration at the edge was avoided by placing the crystal in a 1-inch-diameter hole of a brass collar. The end of the hole was necked down to 15/16 inch diameter and 1/128 inch thickness to retain the crystal and to prevent the edge from being exposed to the water. The crystal was held in place by benzene and polystyrene cement in the area of contact. The collar screwed into a partition so that the tank housing and water-side electrode were at ground potential.

The quartz crystal in the tank is driven at its resonant frequency, 2.603 Mc, by a thermostated crystal-controlled oscillator of the same frequency and a power amplifier (Fig. 3). The thermostated crystal (type JK09, James K. Knight Co.) was found to control the frequency to within a cycle over a period of hours. The voltage applied to the tank crystal was 350 v rms, and the power dissipated in the crystal was estimated to be a few tenths of a watt.

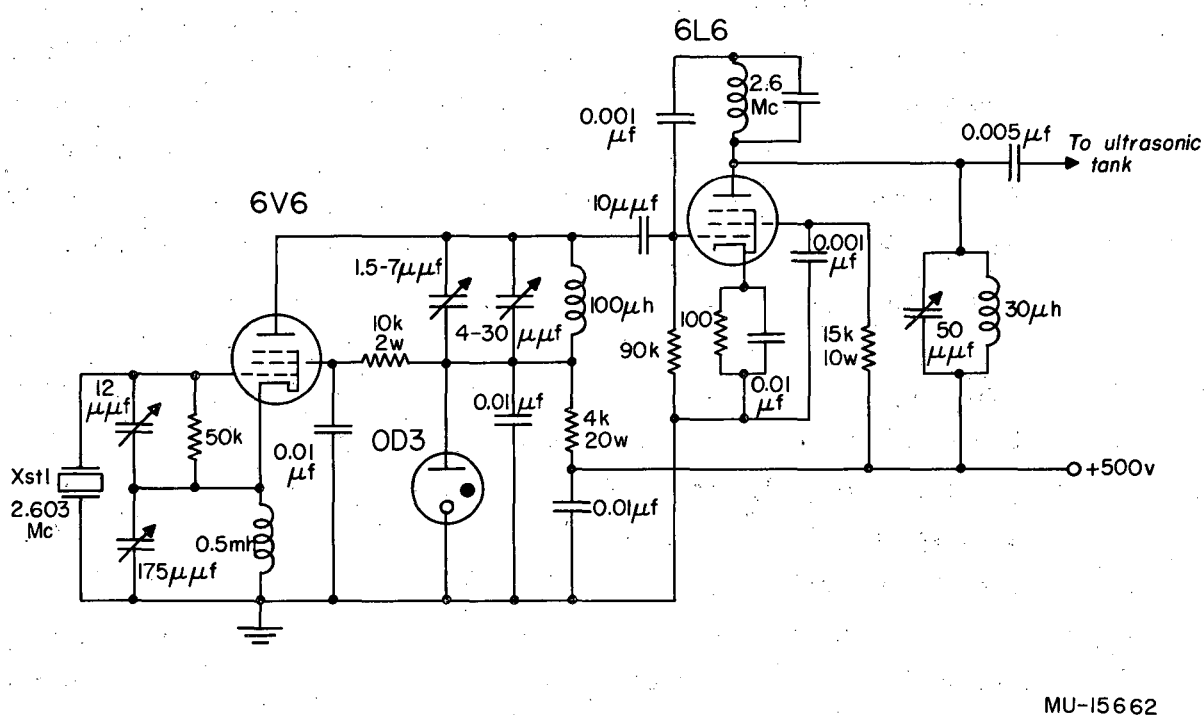

Fig. 3. Power oscillator

For most of the work a mercury A-H4 light source was used, and it was operated on 130 v dc (starting voltage 230 v). If the lamp is run on 60-cycle ac, the slight nonlinearity in the various electronic stages introduces a frequency component that interferes with the desired signal.

The fraction of light modulated ("fraction modulation") was determined by measuring the average dc current I of a photomultiplier exposed to light from slit S_2 (Fig. 2) when there is modulation (I_m) and when there isn't (I_{nm}). The fraction modulation is given by $(I_{nm}/I_m) - 1$, and was found to be 0.05. The low fraction modulation is attributed to the mounting used, which undoubtedly restricted the crystal's motion unnecessarily; it might even have changed its resonant frequency.

The ultrasonic tank is constructed of brass and contains quartz windows. Styrofoam is placed along the walls on the inside to absorb sound which might reduce the fraction modulation. The reflecting plate can be positioned by several adjusting screws, and the best setting can be determined by replacing slit S_2 with a lens of 10 cm focal length and looking at the diffraction pattern on a screen.

Except for the windows, the tank is enclosed in 2-inch-thick stryofoam. This insulation presumably reduces temperature fluctuations which cause a change in the ultrasonic velocity and wave length and the need for frequent positioning of the reflector.

1. Optics

The optics are shown in Fig. 2. The condensing lens L_1 focuses an image of the light source on slit S_1. The light is rendered parallel by lens L_2, passes through the ultrasonic grating, and finally is brought into focus in the plane of S_2.

The fraction of useful light going through slit S_2 was determined by measuring the fraction of incident light transmitted at various stages in the optical train. Measurements were made by using the full light of an AH4 mercury lamp and by reading the current

generated in a Weston photronic light meter. Of the total light given off by the source, L_1 receives a fraction given by its solid angle/4π or 0.0068. The fraction of incident light that is transmitted by S_1 is 0.75; the fraction of that incident on L_2, the tank, and L_3 combined is 0.83; and the fraction of that incident on S_2 is 0.55. Since the fraction modulation is 0.05, the over-all useful fraction of light emitted by the source is 1.2×10^{-4}.

Unfortunately, production of parallel light is necessarily wasteful. Strictly speaking, only one point of the light source produces rays that are parallel to the optical axis. In practice, however, the effective area of the AH4 is 2.4 cm $\times$ 0.24 cm, and these rays can be made approximately parallel to the optical axis. Light from points outside this area are more widely diverging and thus are not useful. Use of a larger or faster condensing lens, therefore, does not increase the amount of useful light significantly.

It should be noted that if light sources with larger areas than the AH4 are used S_1 will become more of a limiting aperture since its slit width should be about 0.1 cm or less to allow separation of the different orders at S_2.

2. Electronic Circuitry

A block diagram of the electronics is shown in Fig. 4. There are two signal channels:

1, the fluorescent channel, which derives its signal from the fluorescent or scattered light, and

2, the reference channel, which derives its signal from a small portion of the exciting light. Both signals are reduced from 5.206 Mc to 1000.2 cycles and placed on an oscilloscope in the form of a Lissajous pattern. The pattern is reduced to a straight line, corresponding to a 0° or 180° phase difference, by adjustment of the reference phase shifter. Substitution of the fluorescer by a $BaSO_4$ sol causes the pattern to open up. The phase change is determined by adjusting the calibrated phase shifter in the fluorescent channel until the Lissajous figure is once again a straight line.

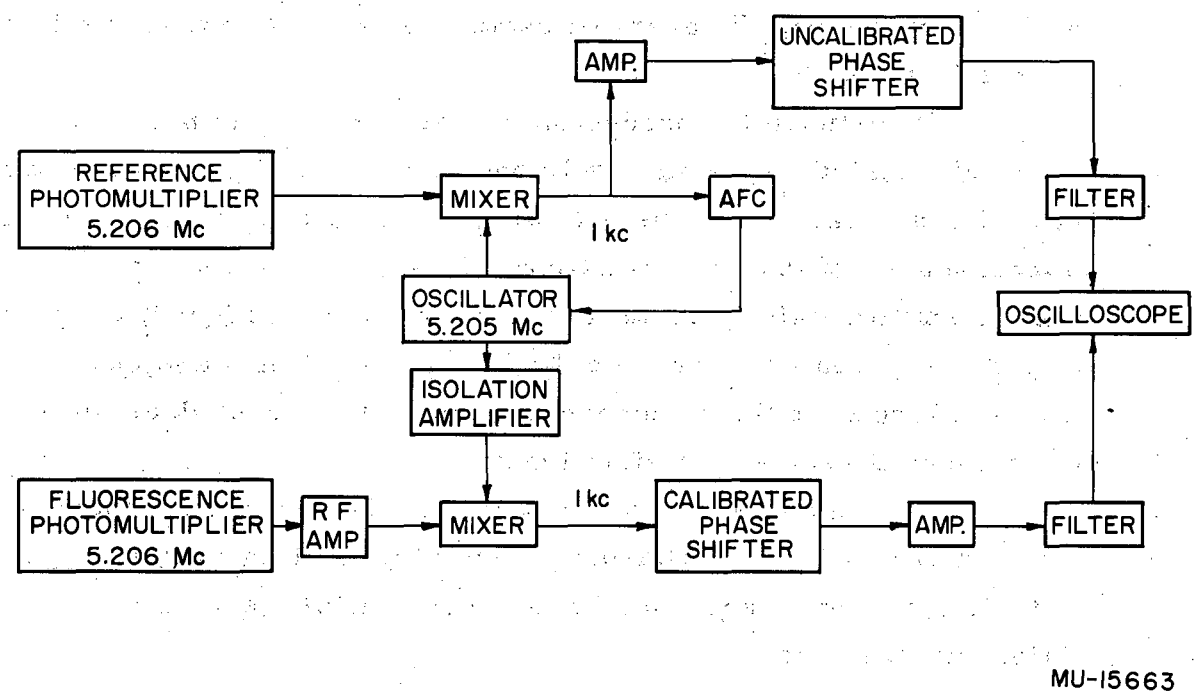

Fig. 4 Schematic of short-lifetime apparatus (electronic circuitry)

In the initial stages of this work, it was hoped that one channel could obtain its signal from a photomultiplier viewing the fluorescent or scattered light, and that the other channel could receive a signal from the oscillator driving the ultrasonic tank. This arrangement was tried but proved impractical because of the large phase changes occurring between the voltage applied to the tank crystal and its motion. The crystal because of its high Q produces a large phase change when the frequency is changed only slightly. When the signals are derived from two photomultipliers, as in the above arrangement, these phase changes go unnoticed.

a. Frequency-reduction unit

Frequency reduction is desirable because accurate phase-shift measurements are more difficult at high frequencies than at low frequencies. Another reason is that the noise of the photomultiplier, which is the limiting noise, can be reduced conveniently by the use of a low-frequency narrow-band-width filter.

The mixer of the reference-signal channel is identical to the mixer in the fluorescent channel, and both are driven off the same beat oscillator (Fig. 5). The output of both mixers is a 1000.2 ± 0.05-cycle signal. The fluorescent-channel low-noise amplifier and mixer is shown in Fig. 8.

To prevent the 5-Mc reference signal from getting into the fluorescent channel, an isolation amplifier (Fig. 5) is used between the beat oscillator and the fluorescent-channel mixer.

Frequency reduction does not alter the phase relationship between two signals. For example, if two signals $\cos(\omega_1 t - \phi)$ and $\cos(\omega_1 t)$ of the same frequency ω_1 and of phase difference ϕ are mixed separately with a third signal $\cos(\omega_2 t)$ of frequency ω_2, the resulting signals will be given by $\cos(\omega_1 t)\cos(\omega_2 t) = (1/2)\cos(\omega_1 + \omega_2)t + (1/2)\cos(\omega_1 - \omega_2)t$ and by $\cos(\omega_1 t - \phi)\cos(\omega_2 t) = (1/2)\cos((\omega_1 + \omega_2)t - \phi) + (1/2)\cos((\omega_1 - \omega_2)t - \phi)$. It is seen that the phase relationship is conserved in the sidebands of the same frequency. In this work the lower-frequency side band $(\omega_1 - \omega_2)$ is retained and the other rejected.

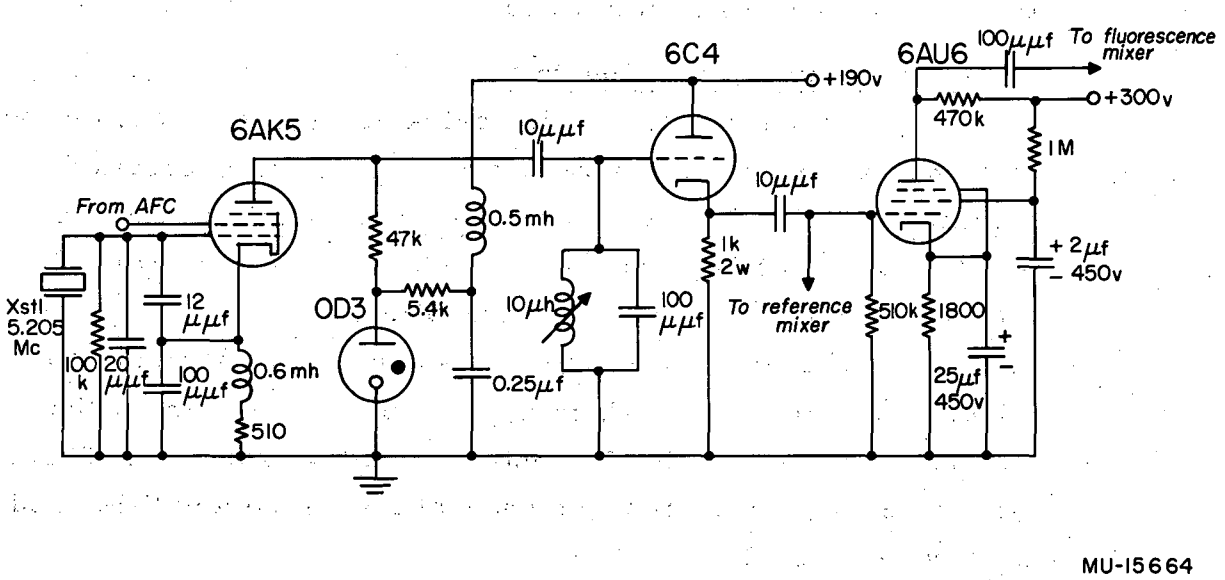

Fig. 5. Beat oscillator, cathode follower, and isolation amplifier

b. Automatic frequency control

An automatic frequency control (AFC) using a phase discriminator, Fig. 6, holds the 1000.2-cycle beat frequency to ± 0.05 cycle or better as determined by a Berkeley Eput meter. With the aid of this control, drift in the beat frequency and the need for constantly determining its value are eliminated. Thus, more accurate measurements can be made and ease of operation is greater.

Frequency control is achieved by placing a 1000.2 ± 0.05-cycle frequency standard across a bridge in quadrature with the 1-kc beat note from the reference channel. When the frequencies are identical and 90° out of phase, the rectified output of the bridge is zero, and a balance results. When the frequencies are different, an imbalance occurs, causing one triode of the 12AT7 to change the screen voltage of the beat oscillator (6AK5). This action results in a change of frequency in the beat oscillator, tending to keep the beat frequency constant at 1000.2 cycles. The frequency of the beat oscillator can be varied up to one cycle, and since the driving oscillator for the tank and the beat oscillator hold to within less than one cycle, the method is satisfactory.

To obtain a 90° phase relationship between the standard frequency and reference signals, a variable RC network was used across the output of the standard frequency signal.

It was found that the AFC did not lock in if the crystal ovens for the beat and tank oscillators were used even though the thermostatic contacts operated properly. Since good control could be obtained without the ovens, they were not used. Also a 500-v regulated power supply for the tank oscillator and power amplifier were used in place of an unregulated supply, since it gave better frequency control.

The frequency standard is a 1000.2-cycle tuning fork (made by the Riverbank Laboratories, Department of Engineering, Geneva, Ill.) whose two coils are in the grid and plate circuits respectively of an oscillator. The oscillator was found to be constant to ± 0.05 cycle or better. The fork possesses a temperature coefficient of one

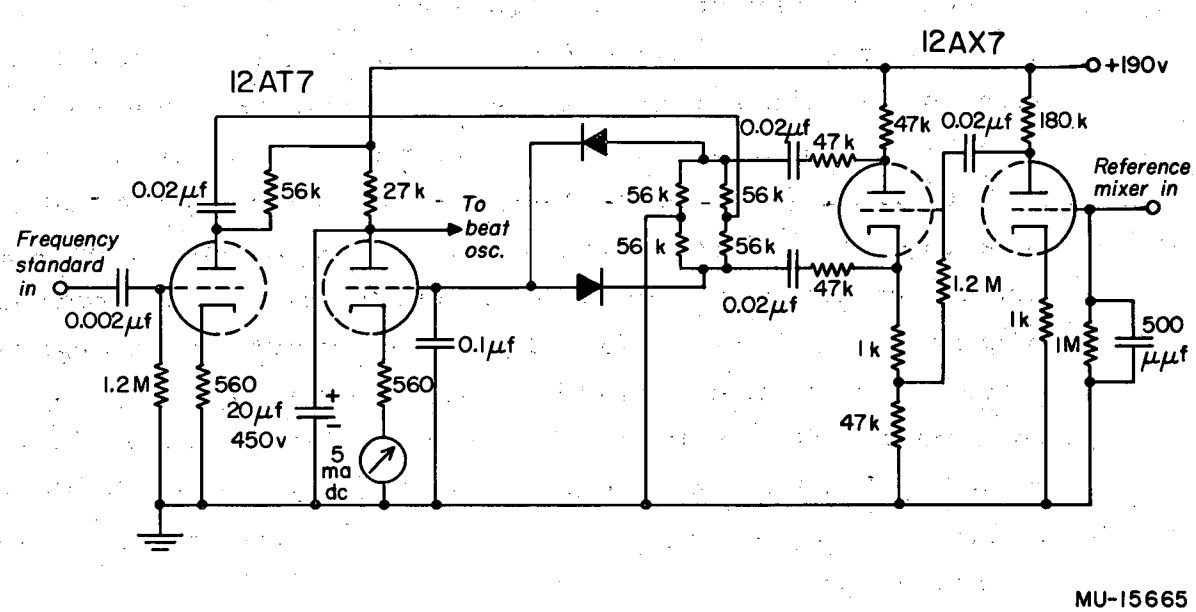

Fig. 6. Automatic frequency control

part per million per ^{o}C in the range 0 to 70° C. Crude measurements indicate its band width is of the order of 0.1 cps. This frequency standard was found to be quite satisfactory, although even better control could be achieved by use of a 100-kc crystal-controlled oscillator whose output is frequency-divided down to 1 kc.

c. Light detector and preamplifier

The light detector is a 6655 photomultiplier having a 1-3/4-inch end-on photocathode. It is operated at 1000 volts. To minimize loss of the 5-Mc signal from the phototube, a cathode follower (6C4) (Fig. 7) is used as an impedance-matching device between the phototube and a low-noise amplifier (Fig. 8). The cathode follower is mounted on the base of the photomultiplier, and both are housed in a hollow aluminum cylinder 3/32 in. thick. A low-noise amplifier (6BQ7), grounded grid type, is used to amplify the feeble fluorescent signals prior to mixing. This action insures that a strong beat note will result and serves to increase the sensitivity of the apparatus.

d. Phase shifter and calibration

The phase shifters in the reference and fluorescent channels are the same in circuitry, but only the fluorescent channel phase shifter is calibrated. The schematic and equivalent circuit for each phase shifter is shown in Fig. 9. The 12 AU7 generates an ac voltage across a variable RC network and the plate and cathode resistors. If the plate (E_1) and cathode (E_2) voltages are 180° out of phase and if they are equal with respect to ground potential, the output voltage E_0 is a vector of constant magnitude with varying phase. From the vector diagram we have $\tan(\phi/2) = R/X_c$. Knowing R and X_c, one can determine ϕ. If ϕ_1 and ϕ_2 are the phase angles corresponding to fluorescent and scattered light respectively, then the desired phase angle is $\phi = \phi_2 - \phi_1$, where $\tan\phi = \omega\tau$ and $\omega = 3.271 \times 10^7$ sec^{-1}. Through these relationships the lifetime τ can be determined.

The cathode and plate voltages were checked with respect to phase by observing their Lissajous pattern, which gave a perfectly

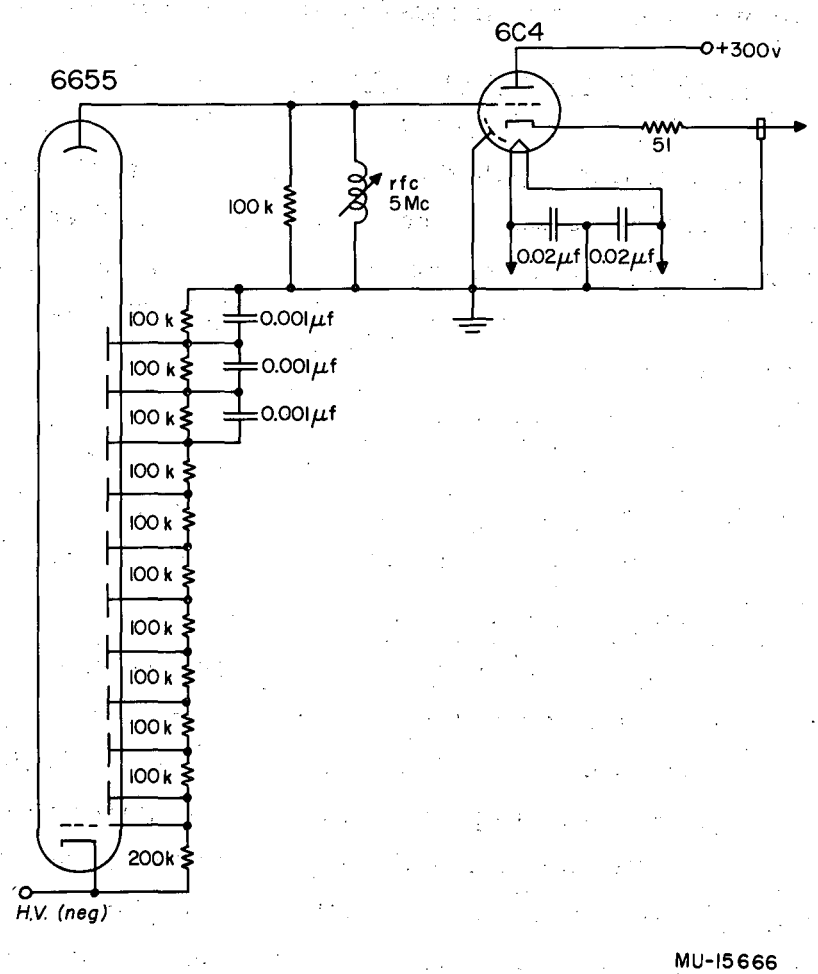

Fig. 7. Photomultiplier and cathode follower

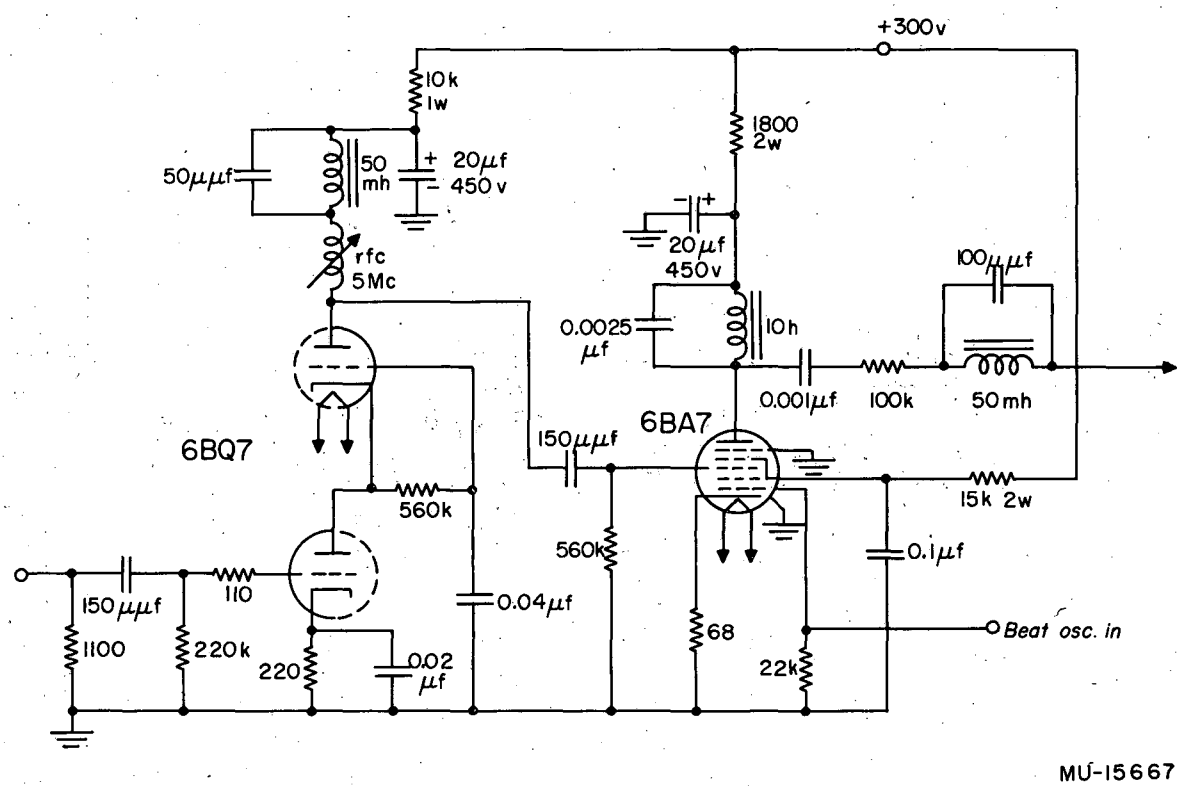

Fig. 8. Low-noise amplifier and mixer

(a).

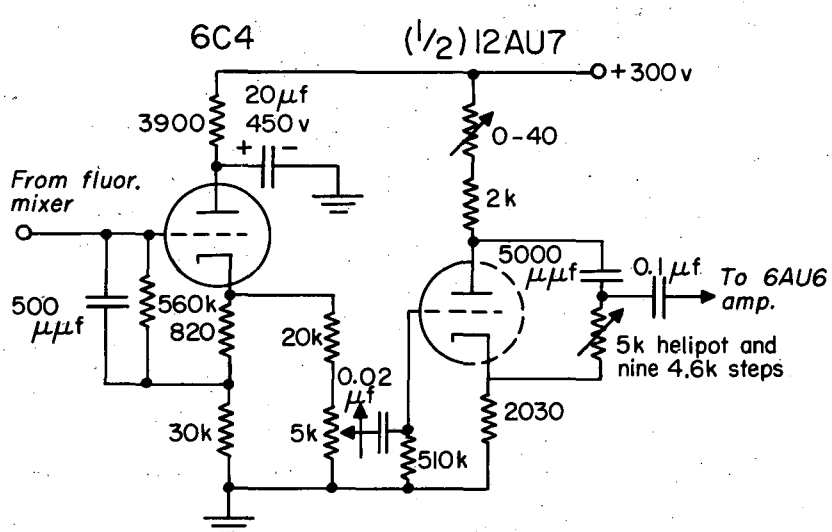

(b)

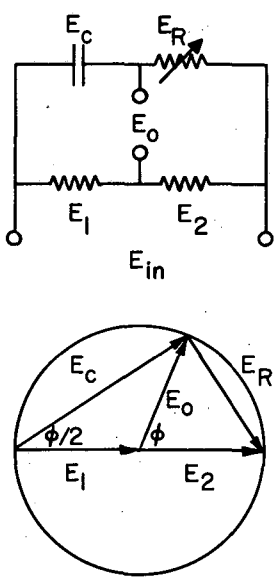

MU-15668

Fig. 9. (a) Cathode follower and phase shifter (schematic); (b) Phase shifter equivalent circuit and vector diagram.

straight line. Under these ideal conditions phase angle can be detected to within 0.3°. A more sensitive test of both phase and amplitude balance was made by using a nulling device. Two 55,888-ohm resistors in series were connected across plate to cathode via two 1-μf capacitors (X_C = 160 ohms), to obtain ac coupling only. When the plate and cathode voltages are equal in magnitude and 180° out of phase, the potential between ground and the midpoint of the two resistors is zero. If the amplitude and phase are not quite in balance a small signal remains. The ratio of the residual signal to the ac plate voltage is a measure of the deviation from the condition of balance. Amplitude adjustments were made with a 40-ohm potentiometer in the plate load. The residual signal observed indicated that the phase and amplitude are balanced to 0.1%.

The effect of the 12AU7 and plate and cathode resistors on the impedance of the RC network was found to be less than 0.2%. The plate resistance of the 12AU7 is 4kΩ, the plate and cathode resistors 4kΩ, and the capacitive reactance 30 kΩ (assuming R = 0). The combined impedance is

$$Z = 2(30) / \sqrt{30^2 + 2^2} = 1.996 \text{ k}\Omega ,$$

which deviates from 2kΩ by 0.2%. As a check on this effect, the null was observed while the value of R was changed from 0 to 40 kΩ. No change in the amplitude of the null could be detected, thus the above calculation was supported.

The effect of output loading on the impedance of the phase shifter was found to be significant to 0.2%. The load consists essentially of a 5 meg grid resistor (6 AU6 circuit). The analysis is the same as that given by Chance et al.[16]

The phase angle is changed by adjusting the resistance R. R can be varied in nine 4.6-kΩ steps each and continuously with a 5kΩ ten-turn Helipot. The fixed resistors are evaporated chromium film type, have a small temperature coefficient of -150 ppm/^{0}C, and are noninductive.

The fixed resistors and Helipot were calibrated with an impedance bridge, Model 250-DA, Electromeasurements, Inc., Portland, Oregon, to an accuracy of 0.1%. The Helipot is reported to be linear to 0.05%, but a slight nonlinearity was found between 0 and 250 ohms. Consequently this region was plotted on a graph. In the linear region 250 to 5000 ohms, a least-squares treatment yielded the relation

$$y = 1.1 + 507.0\,x,$$

where y is in ohms and x is in revolutions of the Helipot. The equation can be used to a probable error of 0.2 ohm, but only to an accuracy of 0.1%, however.

The phase shifter's capacitor was a silver-mica type of approximately 5000 μμf. It was calibrated by means of a General Radio Impedance Bridge, type 650 A, and a General Radio Precision Capacitor type 222-S, which is accurate to 1 μμf in the range 0 to 2500 μμf. Because 5000 μμf is outside the range of the precision capacitor, a 2500-μμf capacitor was calibrated and then added to the precision capacitor in parallel. The value obtained was 4945 μμf, which is accurate to at least 0.1%. The corresponding reactance at 1000.2 cps is 32,178 ohms.

Because the phase shifter attenuates the input signal it is necessary to add a stage of amplification in the reference channel. The circuitry is indicated in Fig. 10.

e. Q-multiplier filter

In order to increase the sensitivity of the apparatus, it is desirable to eliminate as much of the noise as is possible at the phase detector. By far the largest contribution is the noise-in-signal component of the photomultiplier. As is well known, this noise is the result of the statistical nature of photoelectric emission. The mean-square current of the noise-in-signal[17] is given by

$$\overline{i_n^2} = 2e\bar{i}\,\Delta f$$

where Δf is the band width of the entire electronic system, $\bar{i}$ is the average photoelectric signal current, and e is the electronic charge. The signal-to-noise ratio (S/N) is given by

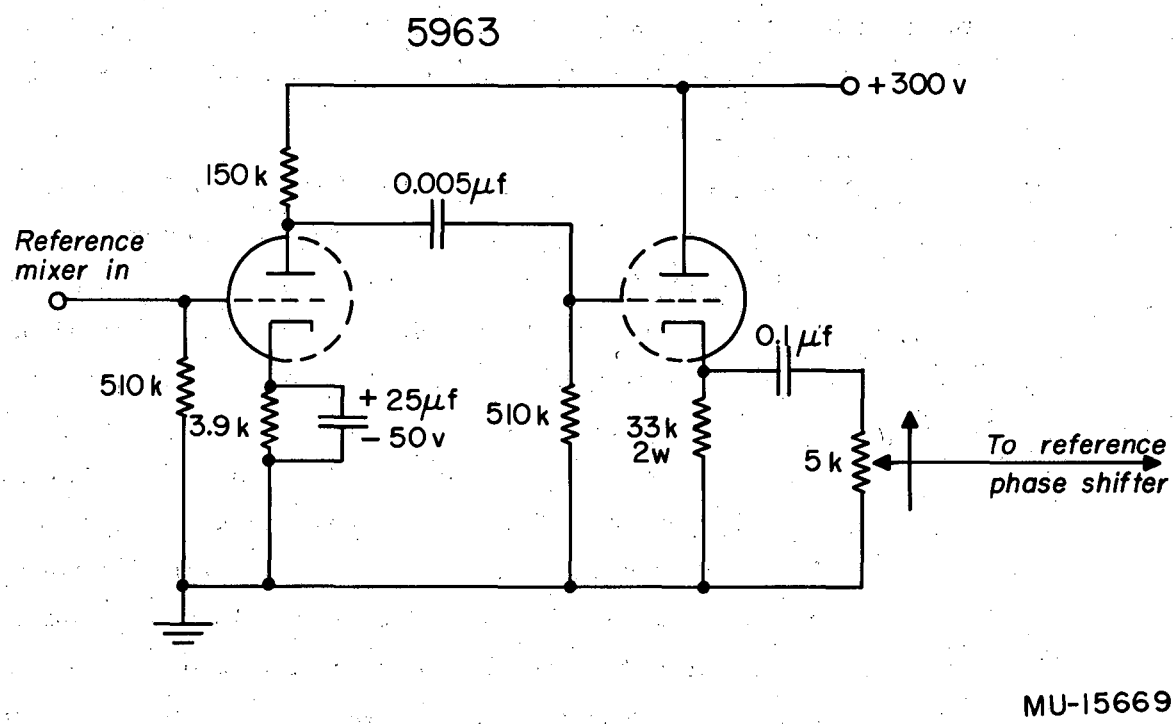

Fig. 10. Reference-channel amplifier and cathode follower

$$S/N = \bar{i}/(\overline{i_n^2})^{1/2} = (\bar{i}/2e\Delta f)^{1/2}.$$

Hence, to obtain a large S/N the amount of light striking the photomultiplier should be large and the band width small. Unfortunately, the signals encountered in these measurements will be small, but the band width can be made small. A Q-multiplier filter, Fig. 11, with a center frequency of 1 kc and a band width of about 4 cycles was used for this purpose both in the reference and fluorescence channels. The band width is sufficiently large, however, so that frequency changes of the order of 0.05 cycle will introduce negligible phase shift.

f. Phase detector

The phase detector consists of forming a Lissajous pattern on an oscilloscope of the 1-kc reference and fluorescence signals. The reference phase shifter is adjusted until the pattern degenerates into a straight line, indicating 0° or 180° phase shift. Substitution of the $BaSO_4$ sol for the fluorescer causes the pattern to open up. The calibrated phase shifter in the fluorescent channel is adjusted until a straight-line pattern appears again. From the initial and final settings of the calibrated phase shifter, the phase angle can be determined.

I feel that this phase detector lacks sensitivity and is actually limiting the accuracy of the measurement. With this phase detector lifetimes could be determined to a precision of 0.7%. A phase detector employing observation of a null of two signals 180° out of phase and of equal amplitude would be preferable.

g. Power supplies

The oscillator (6V6) and power amplifier (6L6) driving the ultrasonic tank are run off a separate regulated power supply. This circuit drew 80 ma at 400 v.

The power supply for the AFC, reference mixer, and beat oscillator is voltage-regulated. It delivers 190 v at 70 ma.

The remaining section of the reference channel is supplied with a Pedersen 300-v supply, which is regulated and has a maximum rating of 2 amp.

The fluorescent-signal channel receives its power from a second Pedersen 300-v regulated supply with a maximum current rating of 2 amp.

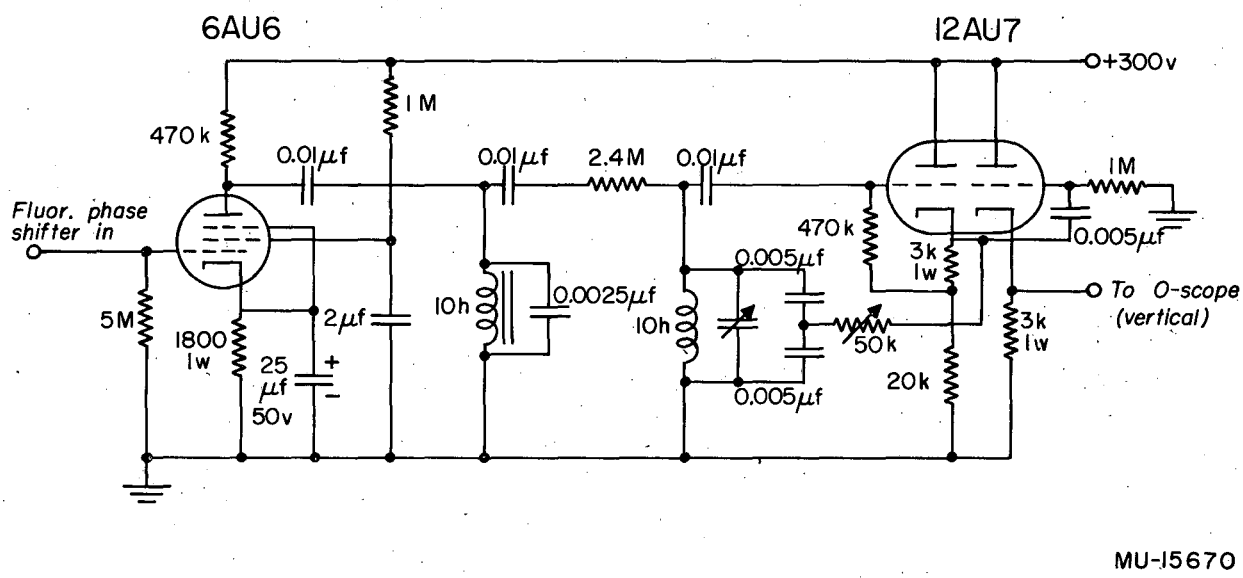

Fig. 11. Fluorescence-channel amplifier and Q-multiplier filter

Both photomultipliers receive 1000 v from a Pedersen Electronics regulated supply rated at 3 kv and 10 ma.

PROBLEMS ASSOCIATED WITH THE PHOTOMULTIPLIER

Although the photomultiplier is unsurpassed in its ability to detect weak light signals, it is severely limited when time measurements are being made in the range of 10^{-8} second or less. One difficulty arises because photoelectrons ejected from different areas of the photocathode travel different distances to the first dynode, and thus have different transit times. Measurements on transit times have been made at the Radiation Laboratory, University of California, Berkeley[18] because of their importance in measuring fast nuclear events. The results show that for flat-faced photocathodes, such as the RCA 6655 photomultiplier, electrons leaving the center of the photocathode arrive at the first dynode 10^{-8} second sooner than those leaving the edge. It will be noticed that 10^{-8} second is a typical lifetime value, and therefore the effect is of considerable importance in lifetime measurements.

A second difficulty peculiar to semitransparent photocathodes arises because about 30% of the incident light is transmitted by the cathode. This light bounces around inside, ejecting photoelectrons from the dynodes or the vacuum side of the photocathode. This effect is not so important as the area effect, but evidently is present, and is difficult--if not impossible--to eliminate without changing the design of the tube.

So far as lifetime measurements are concerned, the photomultiplier produces a signal that is the sum of many signals differing in phase and amplitude but of the same frequency. The resultant signal is characterized by a certain amplitude and phase, and by the same frequency. This point is illustrated by considering the summation of the various component signals, namely,

$$\text{Resultant signal} = \sum_n a_n \operatorname{Sin}(\omega t + \phi_n) .$$

Expanding each sin term and factoring out the sin ωt and cos ωt yields

$$\text{Resultant signal} = p \cos \omega t + q \sin \omega t$$
$$= r \sin (\omega t + \theta)$$

where $\sin \theta = p/r$, $p = (a_1 \sin \phi_1 + a_2 \sin \phi_2 + \ldots)$, $q = (a_1 \cos \phi_1 + a_2 \cos \phi_2 + \ldots)$, and $r^2 = p^2 + q^2$. Thus, the time dispersion of the signal itself in no way alters the accuracy of the lifetime measurement. However, if for any reason the geometry of the light falling on the photomultiplier is changed in a given run, errors in the lifetime of more than 100% can result.

This effect was demonstrated by monitoring light of 5 Mc modulation with two photomultipliers and by observing their Lissajous pattern on an oscilloscope. If one photomultiplier is moved slightly from side to side so that different areas of the photocathode are illuminated, the Lissajous exhibits a large change in phase angle.

The effect was also observed when an attempt was made to calibrate the phase shifter by using the transit time for light traveling a known distance. The distance the light traveled before reaching the photomultiplier was varied by moving a mirror along an optical bench. The light image was about 1/8 inch square and remained so over a distance of 250 cm. The photocathode was masked down to a 1/8-inch-square opening in its center. Under these conditions measurements were far from being reproducible. It was suggested that a scattering agent placed in front of the cathode would help in reproducing the light geometry for different settings of the mirror; however, this idea was never explored.

In view of these results, consideration must be given to whether or not the $BaSO_4$ sol reproduces the effect of the fluorescent substance with regard to light geometry. To test this effect, a 0.008 M $BaSO_4$ sol in 50/50 water-ethanol was prepared, and a number of dilutions were obtained from it down to 10^{-4} M. The different concentrations were compared with respect to differences in phase of the scattered light. The sols were placed in cells 1 inch long and 7/8 inch in diameter. When the incident light was masked

down to prevent light from scattering off the walls or neck of the cell, a bright shaft of scattered light 1/2 by 0.04 by 1 inch could be seen in the cell. For concentrations of sol less than 7×10^{-4} M no difference in phase could be detected. The 0.008 M sol differed in phase from the 7×10^{-4} M one by a few degrees, however. The same results were observed whether the full light of the mercury lamp was used or just the 3650 Å line. The difference in phase angle for the higher-concentration sol is to be attributed to its larger gradient in light intensity. Therefore, a sol whose concentration is less than 7×10^{-4} M would simulate the light geometry of a fluorescing substance provided the latter has nearly uniform brightness along its optical path length.

On the other hand, if the fluorescent substance itself had a high optical density, dilute sols would not reproduce the light geometry. Consequently, lifetimes that are determined by making measurements at high concentration and by extrapolating these data to infinite dilution will be in error if this effect is not considered.

Attention must also be given to where the reference photomultiplier is placed, so that its light geometry is not affected when the fluorescent substance and $BaSO_4$ sol are interchanged. The best procedure is to place the reference photomultiplier ahead of the fluorescent photomultiplier. In this way interchanging the sol for the fluorescer can have no effect on the light geometry. In the present arrangement the reference photomultiplier receives a small amount of modulated light from a mirror placed in a portion of the light beam emerging from S_2. This procedure was considered preferable to using a sol, since less than 10% of the light is intercepted by the mirror, whereas even a dilute sol can reduce drastically the amount of light falling on the fluorescent substance. In addition, the reference photomultiplier receives a more intense signal from the mirror than a dilute sol. Contrary to Bailey's experience, no difficulty was encountered by using a mirror.

A few attempts can be made to minimize the dispersion time in a photomultiplier. One way is to mask down over one-half

the photocathode so that only the central part can be exposed to light. Another method is to increase the voltage between the cathode and the first dynode, since the transit time goes inversely as the square root of the voltage. Finally, the best method is to use a spherical photocathode so that all points on the cathode are equidistant from the first dynode. Spherical cathodes reduce the time dispersion to 10^{-9} second.[18] A few photomultipliers on the market posses spherical photocathodes, perhaps by accident; however, now that the magnitude of the effect is known, a conscious effort is being made by RCA and others to produce the spherical photocathode.

There is no doubt that one of the anomalies that Bailey encountered can be explained by the characteristics of the photomultiplier. In this connection, one serious objection can be raised with regard to his method (and Kremann's also) of determining phase. His phase detector involved determining a null, which in turn required changing the amplitude and phase relation of two signals. The amplitude was changed by the adjustment of two slits in front of the two 1P21 photomultipliers, and thus the light geometry and phase angle could have been altered during a run. Bailey mentions, however, that slit S_2 (see Fig. 3 in his paper) had to be masked down to avoid a phase shift when the photomultiplier slits were opened. Masking slit S_2 reduced the light image in one direction whereas the photomultiplier slits reduced it in the other direction and thus an exceedingly small image was striking each photomultiplier. The obvious disadvantage in their method is that practically all the light must have been wasted. The present arrangement, on the other hand, uses practically all the light coming from slit S_2. With this modification the sensitivity of the apparatus is increased perhaps 100-fold.

SENSITIVITY OF THE APPARATUS

As a guide to future work, the sensitivity of the apparatus was determined. Sensitivity as used here means the minimum brightness temperature of a light source that is required to make a reliable lifetime measurement. A reliable measurement is defined as one for which the signal-to-noise ratio (S/N) at the phase detector is 6 and the optical density of the absorbing gas is low enough to prevent significant self-absorption. The brightness temperature of a substance is defined as the temperature a black body would have if it had the same intensity as the substance at the wave length in question. The advantage of using the brightness temperature is that it actually allows one to determine how many photons per second the source is emitting, whereas the equilibrium temperature does not. A fuller discussion of these considerations and a list of recently determined brightness temperatures for various sources are given in the thesis of Earl F. Worden.[19]

The minimum brightness temperature needed to make a measurement was obtained first by determining the number of photons per sec striking the photomultiplier when a S/N of 6 was observed at the phase detector. This condition was achieved simply by decreasing the amount of light falling on the photomultiplier until a S/N of 6 was observed. The anode load was then replaced by a 10-meg resistor, and the modulator was turned off. The voltage drop across the resistor was observed on an oscilloscope thereby allowing dc voltages to be measured. With an anode-supply voltage of 1000 v, the dc voltage observed corresponded to a current of 5×10^{-8} amp. Since only 5% of the current measured can be modulated, the amount of useful current was 0.25×10^{-8} amp.

To proceed further, consider an experiment in which one of the sodium D lines is used to excite sodium vapor, and the resonance transition is observed in emission. To convert anode current into the corresponding number of photons/sec striking the photomultiplier, the current amplification and quantum efficiency at the photocathode must be known. These quantities were measured at the U. C. Radiation Laboratory for the particular RCA 6655 photomultiplier in use. For

1000-v anode supply v the gain of the tube was 10^6, and the quantum efficiency at the peak spectral response at 4400 Å was 0.125. In other words, 12.5% of the incident photons are converted into electrons. Using this absolute value at the peak sensitivity and the RCA plot of relative sensitivity versus wave length, one obtains a quantum efficiency of 3.4% for sodium D light at 5890 Å.

The minimum number of photons/sec at 5890 Å striking the photocathode that would be required for measuring the lifetime is $(0.05)(5\times10^{-8}\times6.2\times10^{18})/(10^6\times0.034)$ or 4.5×10^5 photons/sec of modulated light. Using this value and the known efficiency of the optics, one can determine what brightness temperature of the source is required. Proceeding in this way, one estimates that about 1/6 of the fluorescent light strikes the photomultiplier. To avoid significant self-absorption the optical density of the gas should be low enough so that only 1/10 (or less) of the incident light is absorbed. Finally, it was shown previously that of all the light emitted by the source the fraction 1.2×10^{-4} of modulated light will be incident on the vapor. These factors yield a value of 4.6×10^{12} photons/sec being emitted by the source in all directions.

The brightness temperature is found through the use of Planck's law,

$$d(E/V) = \frac{8\pi\, h\nu^3}{c^3} \frac{1}{e^{h\nu/kT}-1}\, d\nu, \tag{5}$$

where d(E/V) is a differential energy density for radiation over the frequency interval $d\nu$ under equilibrium conditions. The light source is in a steady state and not in an equilibrium, however; hence, the energy density is 1/2 that given in Eq(5). The power dissipated by the source is c (area of source) d(E/V). If the power is divided by $h\nu$, the units will be photons/sec, and (5) becomes

$$\text{Power} = 4\pi \frac{\nu^2}{c^2} \frac{1}{e^{h\nu/kT}-1}\, d\nu \text{ (area)}. \tag{6}$$

The effective area of the source was taken as 0.6 cm^2, which was the

value obtained for the A-H4 mercury lamp; $d\nu$ was taken as the Doppler width,

$$\Delta\nu_D = \frac{2(R\ln 2)^{1/2}}{c}(\nu)(T/M)^{1/2}, \tag{7}$$

of the sodium line at 109°C, corresponding to a convenient low pressure, 2.6×10^{-10} atmos, for preventing self-absorption. Equating (6) to 4.6×10^{12} photons/sec and solving for T, one obtains a brightness temperature of 1840°K. If the light flux were underestimated by a factor of ten, the temperature would be 2200°K. A factor-of-ten uncertainty in the flux is considered to be a reasonable estimation of the error involved. Since the brightness temperature of a Pirani sodium lamp is about 4300°K for each D line,[19] a lifetime measurement for sodium and various other atoms should be possible. It should be noted that the 2200°K value is supposed to represent a typical case with the present apparatus for a resonance transition. However, a lower temperature could be obtained if the percent modulation were increased and if the wave length of fluorescent light matched the peak sensitivity of the photocathode.

The feasibility of measurements in molecular-gas-phase systems is even more promising in some respects. If the transition for an atomic line and a rotational line are the same with respect to transition probability, degeneracy, population, and wave length, the intensity will be the same in the two cases. In contrast to atoms that possess a single line or a few lines in a narrow wave-length region, molecules possess many rotational lines, and consequently, molecules are capable of giving much larger signals than atoms. In the extreme case in which the spectrum is continuous, the largest signals of all can be expected; this situation would correspond to the large organic molecules such as acridone.

The question might be raised whether each excited rotational level has the same lifetime. So far as the molecular wave function is separable into electronic and nuclear wave functions,[20] the lifetime of each excited state is the same. Therefore, if the signals are weak, one could observe an entire sequence of band heads and feel that within a first-order approximation the lifetime for each excited state is the same.

One of the more promising molecules for lifetime measurements is the CN radical. A convenient light source in this case would be a carbon arc burning in a nitrogen atmosphere. This source produces the violet CN emission in its plasma at a brightness temperature of 5500°K at the band head of maximum intensity, 3883 Å.[19] The minimum brightness temperature of a light source at 3883 Å that would allow a lifetime measurement to be made is 3150°K. This value is obtained by the use of Eq. (6) and the minimum number of photons/sec, $\sim 4.5 \times 10^5$, needed to make a measurement. The calculation assumes the same line width for CN as was used for sodium and the same photocathode efficiency. The ratio of the intensity of a light source at 5500°K to one at 3150°K is $10^{2.1}$, corresponding to a light flux $10^{2.1}$ times the minimum required to make a measurement. This value is a lower limit, however, since the CN band-head is considerably broader than the 5890 Å line of sodium at 109°C.

THE LIFETIME OF ACRIDONE: A DISCUSSION OF ERRORS

Of all the molecules investigated by Bailey or Kromann, acridone was the only one whose lifetime was independent of concentration. Hence, self-absorption is not significant, and the need for extrapolating the lifetime to infinite dilution is avoided. Because of these advantages and the desirability of repeating one of their determinations, the lifetime of acridone was measured.

Eastman Kodak Company acridone which had been recrystallized three times from glacial acetic acid by Kromann was used. A saturated aqueous neutral solution was prepared and placed in a quartz cell 1 inch long and 7/8 inch in diameter. A 7×10^{-4} M $BaSO_4$ sol in 50/50 water-ethanol was used as the scattering agent and was placed in a second cell of the same dimensions. The remainder of the optics were essentially glass, but allowed a sufficient transmission of the exciting light, the 3650 Å mercury line. A small portion of light from slit S_2, Fig. 2, was reflected by a 45° mirror onto the reference photomultiplier. The remaining light passed through a Corning filter #5840, which passed only the 3650 Å line. The exciting light entered an enclosure by means of a narrow opening in its side, passed through the acridone or sol, and emerged from an exit opening on the opposite side of the enclosure. The entrance to the enclosure was masked down to prevent exciting light from hitting the neck and walls of the cell. With these precautions virtually no exciting light reached the photomultiplier, and the need for a light filter in front of the photomultiplier was avoided. The measurements were carried out with the acridone solution at room temperature, and the solution was air-saturated.

The results of these measurements and the values obtained by Bailey and Kromann are listed in Table I. To the author's knowledge no other lifetime determinations have been made for acridone.

The errors associated with the calibration of the phase shifter are of the order of a few tenths of a percent in the lifetime. However, lifetime measurements are not dependent on an absolute phase-angle determination but rather on a difference in two phase angles; thus the errors tend to cancel.

Table I

The fluorescence lifetime of acridone according to different investigators

Author	Lifetime (10^{-8} sec)
Bailey	1.59 ± 0.01
Kromann	1.452 ± 0.005
This work	1.50 ± 0.01

In this work the precision is limited by the sensitivity of the phase detector. If a more sensitive phase detector were used, such as a nulling device, the accuracy of the measurement should presumably be limited by errors associated with optical problems rather than calibration errors. For example, one might question how closely the sol simulates the fluorescent substance with respect to the geometry of the light falling on the photomultiplier. Although Kromann's velocity-of-light measurement might have been correct, at best it is a check only on the calibration of his phase shifter and not on his lifetime measurements.

Table I indicates that each investigator claims an accuracy of 1% or better, but they differ from each other by 3 to 10%. Part of the discrepancy can be traced most likely to a calibration error in Bailey's phase shifter. There are three reasons for believing this to be the case: (a) phase shifting was done at a frequency of 5 Mc, where stray capacitances can introduce significant errors, (b) the calibration was based on knowing the characteristics of a vacuum tube in the phase-shifter circuit, and (c) Kromann's measurements are consistently about 8% lower--where measurements have been repeated--than Bailey's, indicating that the discrepancy is not a random error. If Bailey's value is discarded, this work and Kromann's agree to within 3%, which is probably the best measure of the uncertainty involved in this technique.

LONG-LIFETIME APPARATUS; LIGHT MODULATOR

The long-lifetime apparatus is fundamentally the same as the short-lifetime apparatus, but the difference in modulation frequency requires a different modulator and different associated electronics.

The light modulator consists of an aluminum wheel, 10 inches in diameter and 0.4 inch thick, with 500 V-shaped wedges per inch, pointing out (radially) on its rim. A set of alternate dark and light lines on a slide are imaged onto a 0.4-by-0.4-inch area of the rim so that a pair of lines just covers one wedge. As the wheel rotates, the direction of reflection of light from the rim changes periodically. Reflected light seen from any particular direction in the plane of rotation will be changing its intensity periodically, and hence the light is modulated.

The glass optics shown in Fig. 12 consist of a light source, a set of condensing lenses, a slide 2-by-2-inch with 100 pairs of white and dark lines per inch, a projection lens, and a lens for collecting the modulated light. All of the optics are mounted on a Central Scientific optical bench. The condenser gathers light from the source and images it on the projection lens. The slide placed near the condenser is imaged by the projection lens onto the rim of the wheel; the size of the image is reduced by a factor of five so that there are now 500 pairs of lines per inch.

The projection lens should be of good optical quality to avoid any distortion of the slide's image on the wheel. Its aperture should be large enough to receive all the light coming from the condenser and yet not obstruct the reflected light from the wheel. A compromise between these requirements, the need for a lens of proper focal length, and availability resulted in the use of a Jena Tessar F 2.8 of 5 cm focal length.

The slide was prepared from a drawing on a paper 2 by 3 feet. The negative of a photograph of these lines constituted the slide.

The wheel is driven by a Bodine universal motor rated at 1/3 hp and 10,000 rpm. The wheel is connected to the motor through a spindle (Fig. 13) which is designed to minimize wobble. In the spindle, one matched pair and a single angular-contact bearing No. 206

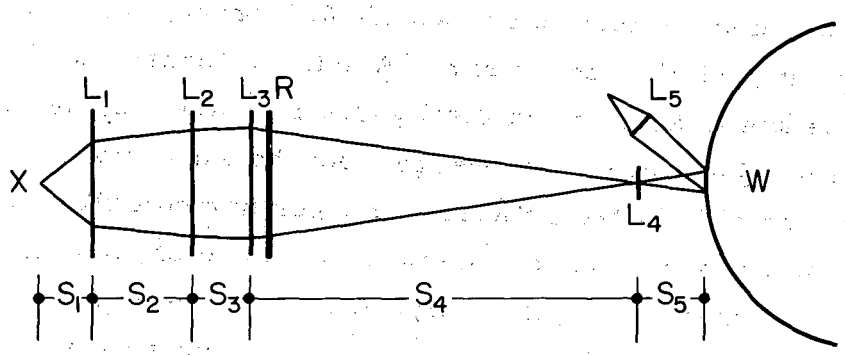

X	*A-H4 Mercury arc*	$S_1 = 4$ cm
R	*Slide with 100 lines/inch*	$S_2 = 7.6$ cm
W	*12.7 cm radius wheel*	$S_3 = 4.5$ cm
L_1	*Glass lens, focal length 16.5 cm, 11.4 cm diam.*	$S_4 = 30$ cm
L_2	*Glass lens, focal length 15.2 cm, 11.4 cm diam.*	$S_5 = 5$ cm
L_3	*Glass lens, focal length 23.1 cm, 11.4 cm diam.*	
L_4	*F 2.8/5.0 focal length Tessar*	
L_5	*Glass lens, focal length 10 cm, 2 cm diam.*	

MU-15671

Fig. 12. Long-lifetime modulator unit

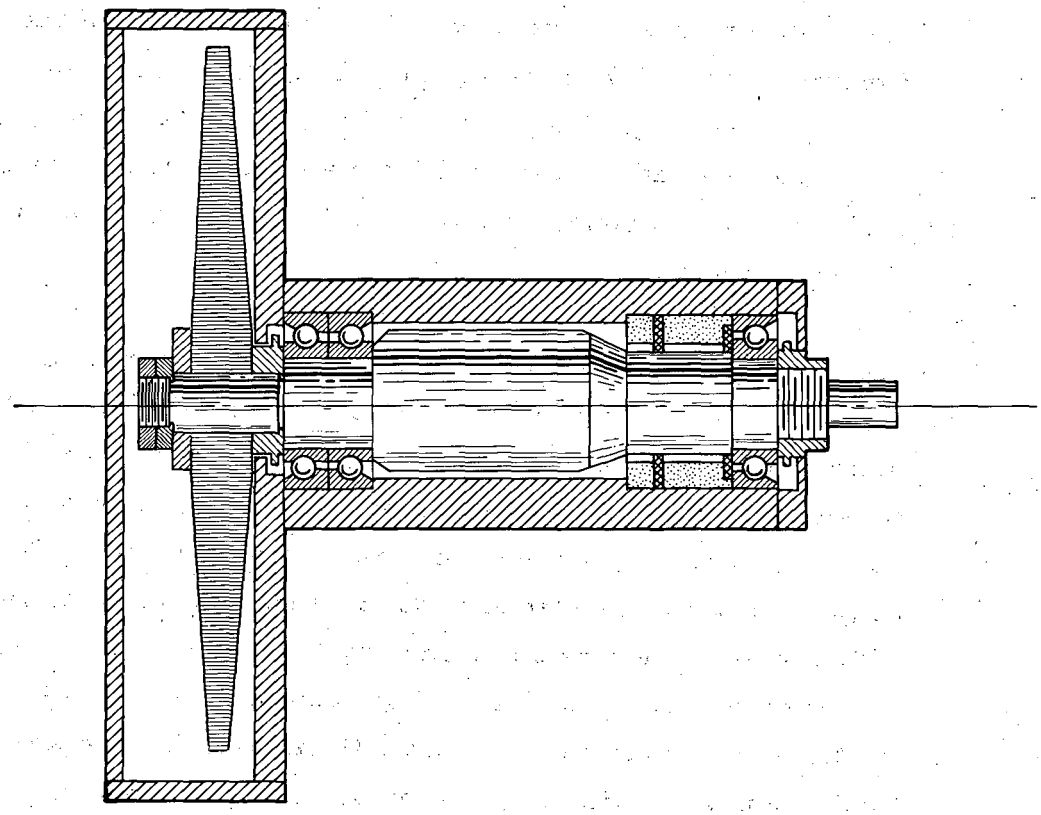

MU-15672

Fig. 13. Wheel modulator and spindle

of precision ABEC-7, were used. In testing the modulator between 5,000 and 10,000 rpm these precision bearings were essential for preventing wobble. Initially, the wheel was to be run at 10,000 rpm, corresponding to a modulation frequency of 2.6 Mc. This idea was abandoned when it became evident that too much time was being spent trying to maintain the spindle and motor in operating condition at high speed. A few of these problems were arcing of the brushes to the commutator, overlubrication or underlubrication of the spindle, and dynamic instability in the motor. Operation below 4000 rpm was satisfactory, however. Operation of the motor at 240 rpm, corresponding to 60-kc modulation, allows lifetime measurements to be made between 10^{-5} and 10^{-7} second, a range which supplements the short-lifetime measurements.

The image of the slide on the wheel must be reduced to exactly the right dimensions, otherwise modulation cannot occur. The size is controlled by movement of the slide and the projection lens along the optical bench. The projection lens can be moved small distances by screwing it in or out of its holder. The slide is in a jig which can be rocked to obtain alignment in the plane of the slide. The slide and the projection lens are placed about 30 and 5 cm respectively from the rim of the wheel, and are positioned by trail and error until modulation is observed by eye. Modulated light can be seen if the jig is moved vertically by means of a screw adjustment. A fine adjustment can be made then by maximizing the output of a photomultiplier which is monitoring the modulated light.

The efficiency of the optics was determined. The relative amounts of light in various places in the optics were obtained by reading the current of a photomultiplier monitoring the dc light. The following results were obtained: one-half the light falling on the projection lens is not transmitted simply because its aperture is too small; only one-fourth of the light reflected off the wheel can be collected, partly because the projection lens is in the way of the reflected beam and partly because of light scattering by the wheel; one-half the incident light on the photomultiplier is modulated. The fraction of light the condensing lenses receive from all the light emitted by the source

is calculated to be about one-tenth. Thus, the useful fraction of light emitted by the source is 6×10^{-3}.

A. Electronic Circuitry

A block diagram of the circuitry is given in Fig. 14. In general, much of the circuitry used for the short-lifetime apparatus is used in the long-lifetime apparatus as well. The fluorescent-signal channel is the same as the circuitry used in the short-lifetime measurements, and consequently, the calibration of the fluorescent phase shifter and the method of determining phase are the same. Therefore, this circuitry need not be described again. The light-detector circuitry is the same as that shown in Fig. 7, and the reference phase shifter is given in Fig. 9. The reference amplifier and cathode follower are given in Fig. 10, and the reference Q-multiplier filter in Fig. 11.

The reference signal is obtained from a photomultiplier viewing modulated light from the wheel. The same signal is used to drive a motor-speed control (MSC) which keeps the 60-kc modulation frequency constant to within 1 cycle. Both fluorescent and reference signals are reduced from 60 kc to 1 kc by mixers and a common beat oscillator, Fig. 15. The reference mixer is the same as that shown in Fig. 8. The beat frequency, about 1 kc, is held constant to within 0.2 cycle by an automatic frequency control.

1. Automatic Frequency Control

Frequency control is accomplished through use of a phase discriminator (6BN6), Fig. 16. Two signals derived from the same 1-kc reference signal, but differing in phase, are applied to separate grids of the 6BN6. The tube conducts only when both grids are positive, and thus the phase difference determines the net output. The phase difference is dependent on the frequency of the signal and the RC coupling network between the mixer and the 6BN6. When the output of the 6BN6 is minimum, a condition of balance is achieved, and the frequency tends to be constant.

The output of the phase discriminator is dc amplified and fed into an increductor whose inductance is dependent on the amount of current flowing through it. The increductor is part of the beat oscillator's

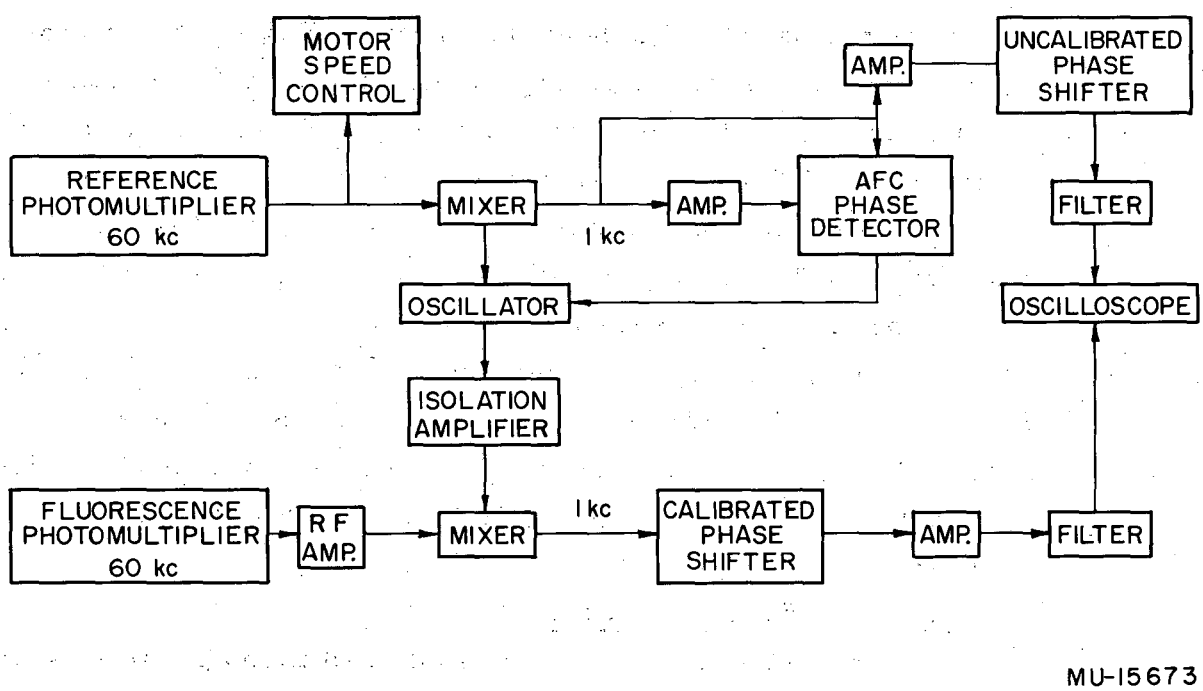

Fig. 14. Schematic of long-lifetime apparatus (electronic circuitry)

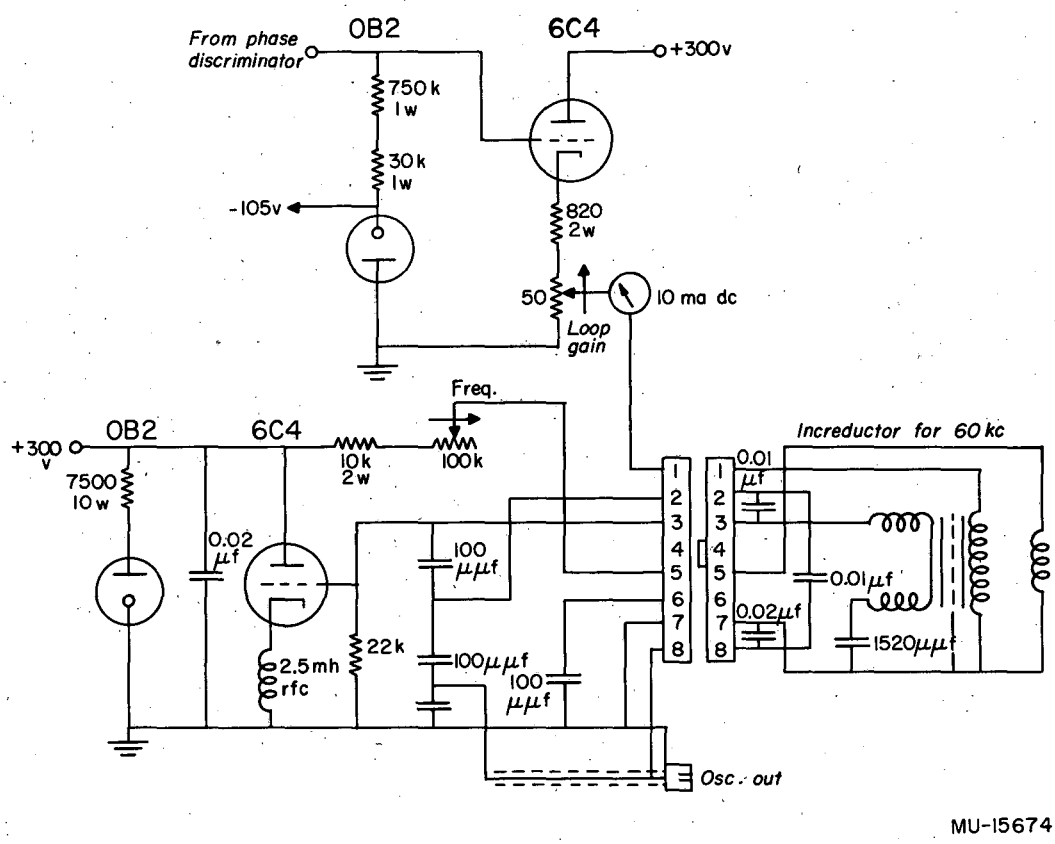

Fig. 15. dc Amplifier of AFC and beat oscillator

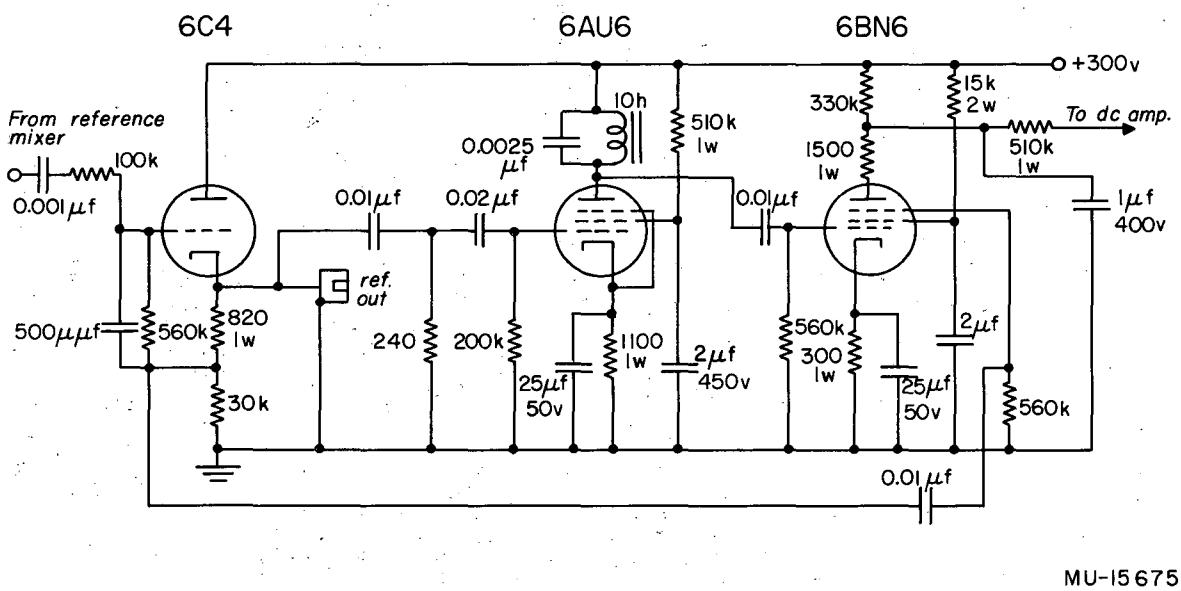

Fig. 16. Automatic frequency control: cathode follower, amplifier, and phase discriminator

grid circuit, so that a change in its inductance results in a change in the radio frequency of the oscillator. Thus, the beat frequency changes correspondingly, and in this way is driven towards a stable condition.

The difference frequency itself can be set to any desired value within the 1-kc range, however. This feature is an inconvenience, since the frequency must be measured accurately each time a phase measurement is made.

2. Motor-Speed Control

The block diagram for this control is represented in Fig. 17. The signal from the reference photomultiplier, following amplification and limiting (Fig. 18), is fed into a conventional frequency discriminator, Fig. 19. The output is dc amplified and power amplified. The power amplifier (Fig. 20) is in series with the armature winding of the motor and a manually controlled dc voltage supply. The field windings are run off a second dc supply, also manually controlled. When the modulation frequency is the same as the center frequency--60 kc--of the frequency discriminator, there is no dc output. When the frequency is different, a dc output results, causing the wheel to speed up and attain the lock-in frequency.

Operation of the MSC at high frequencies is conveniently achieved by reducing the photomultiplier signal from a megacycle or so to 60 kc. For this purpose, a mixer and crystal oscillator can be switched into the circuit as shown in Fig. 21.

B. The Fluorescence Lifetime of Iodine Vapor

The fluorescence lifetime of iodine has been of interest for more than 20 years.[21,25] Most of the work has centered around the efficiency of quenching and of energy transfer of the excited molecule in the upper state of the visible band system. Probably the reason so much attention has been given iodine is that the quenching and energy-transfer efficiencies are large. The quenching is associated with an induced predissociation. The efficient energy transfer to colliding molecules is explained qualitatively by the fact that the separation between neighboring rotational and vibrational levels in the excited state is small and that transitions involving small jumps in energy are the most probable.[22]

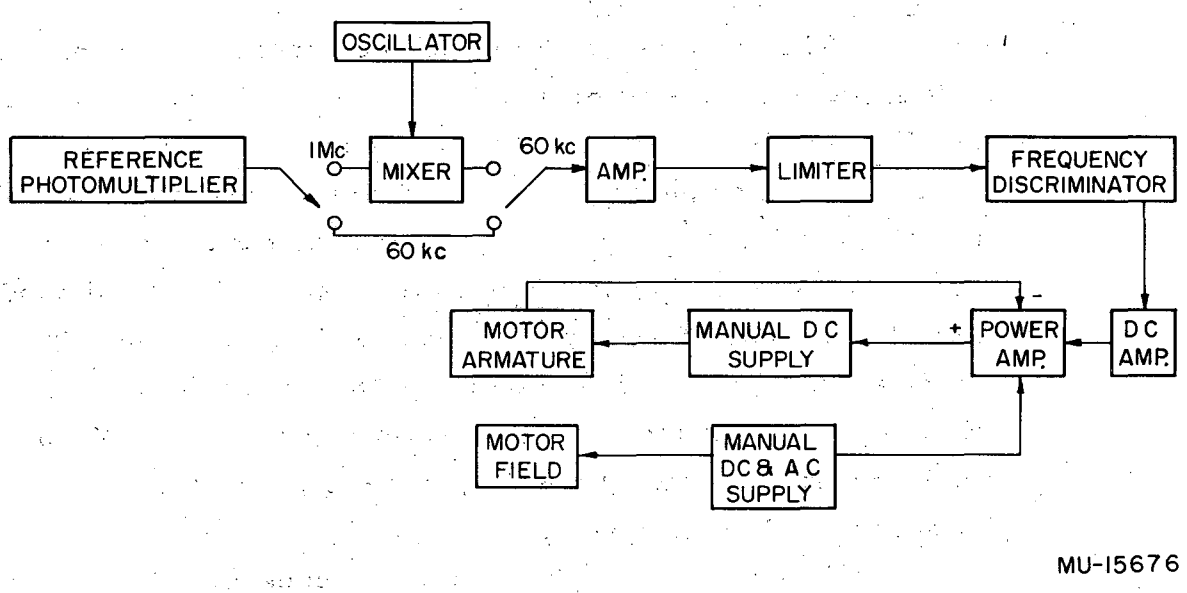

Fig. 17. Motor-speed control schematic

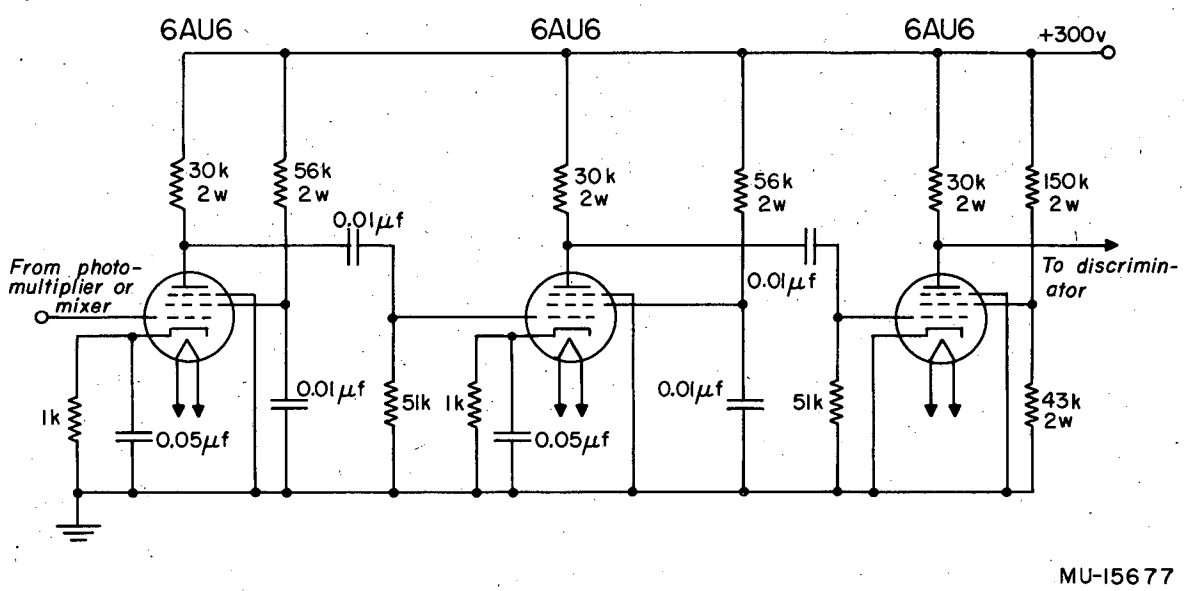

Fig. 18. Motor speed control : amplifiers and limiter

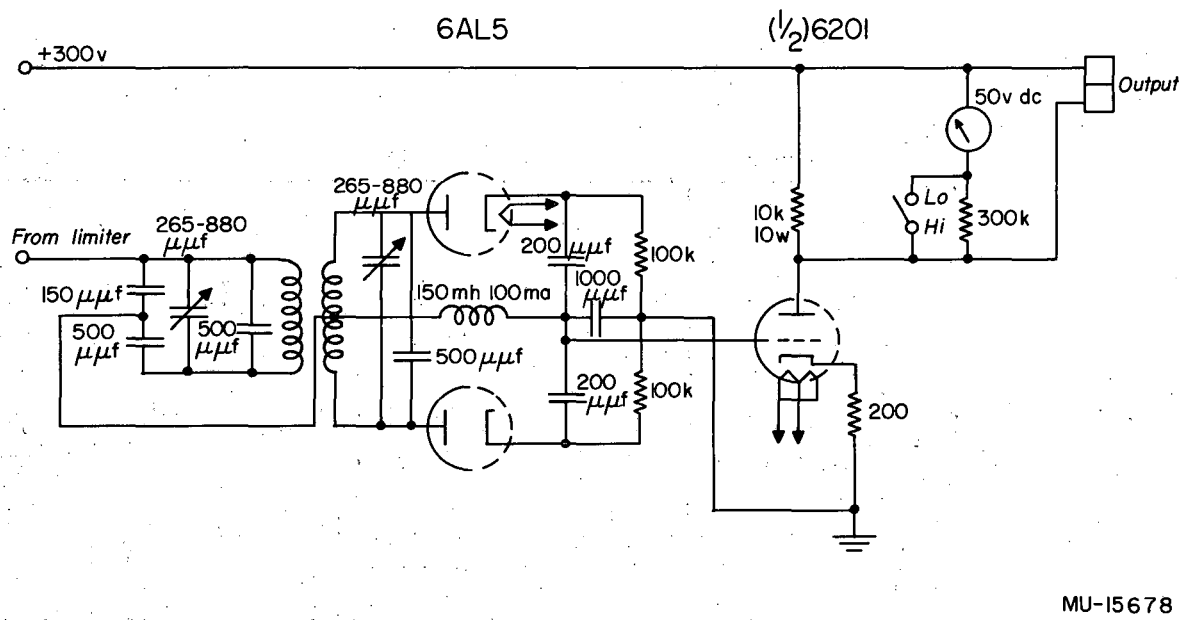

Fig. 19. Motor speed control frequency discriminator and dc amplifier

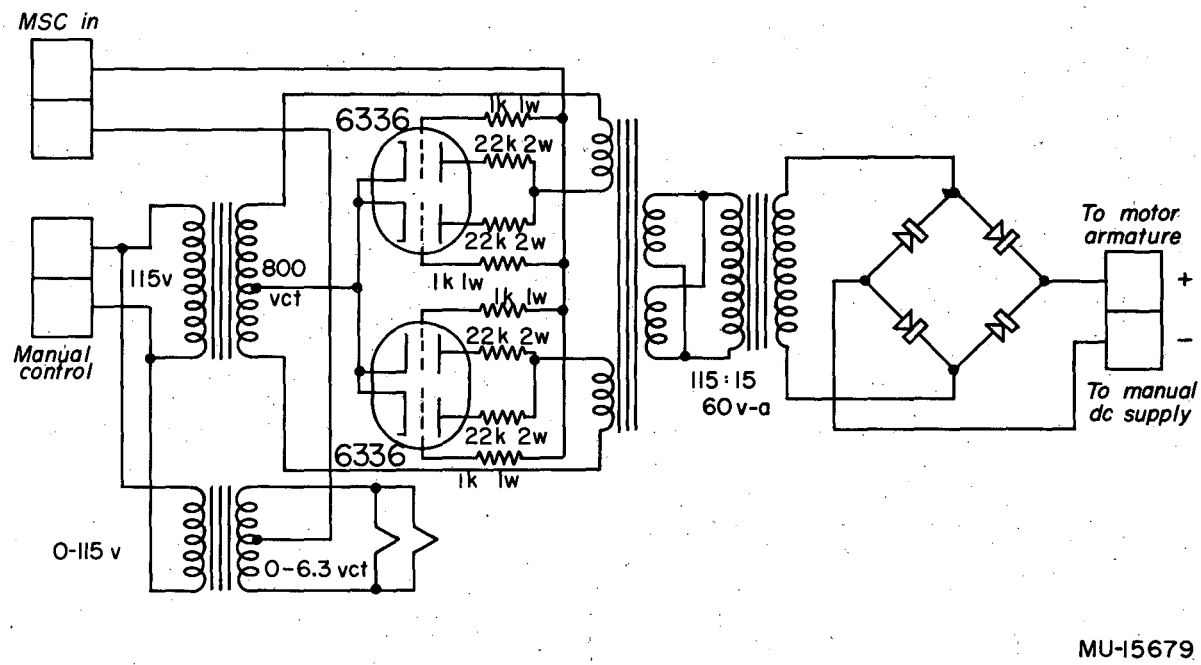

Fig. 20. Motor-speed control power amplifier

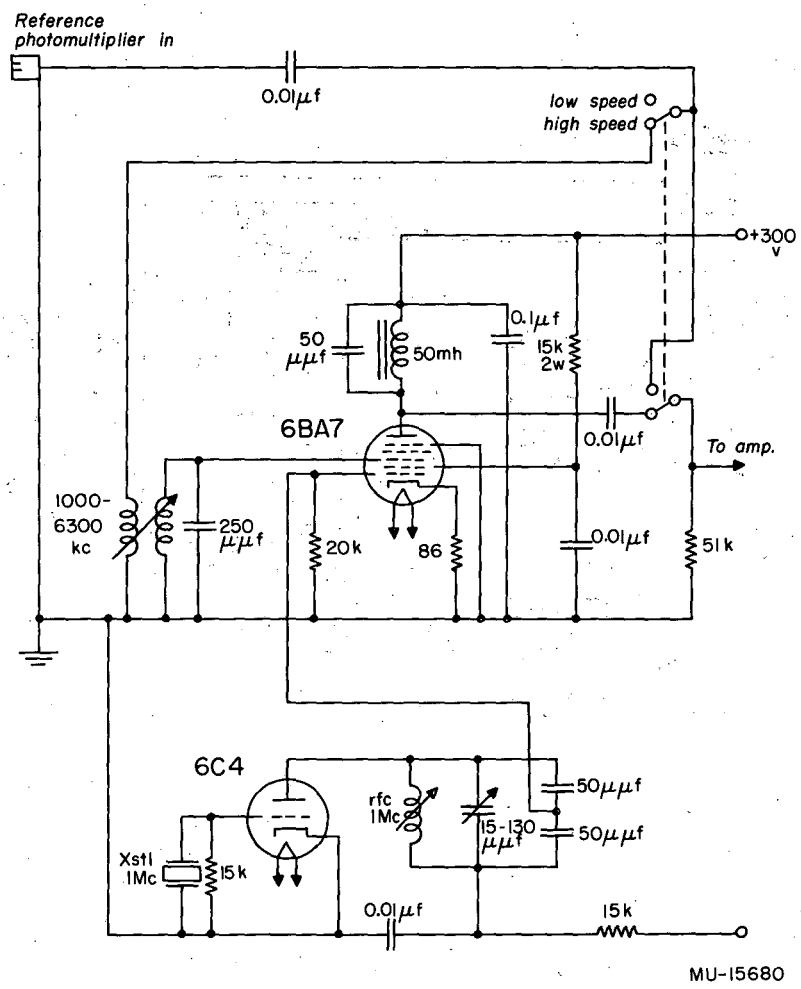

Fig. 21. Motor-speed control mixer and beat oscillator (to be used for 1-Mc modulation)

If the lifetime of the molecule in the excited state is long compared with the time between collisions and if the probability for quenching or energy transfer is high, the intensity of fluorescence will decrease markedly with increasing pressure. This idea is stated more succinctly in the Stern-Volmer expression

$$I = I_0/(1 + \alpha Z t), \tag{8}$$

where I_0 is the fluorescence intensity with no collisional deactivation, I is the intensity with deactivation, Z is the average time between collisions and varies inversely as the square of the collision diameter, and α is the fraction of collisions that result in quenching or in energy transfer. Various investigators have measured I/I_0 and assumed a value for τ and for the collision cross section in order to calculate α. Alternatively, others have assumed a value for τ and a unit collision efficiency ($\alpha = 1$) in order to calculate a cross section. Assuming a τ of 10^{-8} sec, Rossler has reported[23] an effective collision radius for iodine itself of 20 Å, which is considerably larger than the gas-kinetic cross section. Although large cross sections are known for other molecules, the question can be raised whether the correct lifetime was assumed. Wood and Rabinowitch showed that when iodine is in the presence of a few hundred mm of foreign gas, corresponding to a collision time of 10^{-10} sec, the same amount of dissociation occurs whether the exciting light raises I_2 to above or below its dissociation limit in the excited state.[24] Assuming a lifetime of 10^{-7} sec, they showed that every collision results in a dissociation.

More recently, Polanyi has reported collision efficiencies for vibrational energy transfer of excited iodine molecules in the presence of foreign gases such as D_2 and H_2.[25] Assuming a lifetime for the excited state of 3×10^{-7} sec, he finds that vibrational transfers do occur out of one collision in 55 for H_2 and one in 11 for D_2. In the same periodical, Arnot and McDowell report that the ratio of the rate constant for vibrational energy transfer to the rate constant for fluorescence is ten times that predicted by collision theory if a value of 10^{-8} sec is assumed for the lifetime.[26]

Pringsheim in his book "Fluorescence and Phosphorescence"[2] gives an excellent review of the past work on iodine. He mentions that although several different techniques have been used in an attempt to measure the fluorescence lifetime, none of these is reliable, and at best give an upper limit of 10^{-6} sec. In view of this uncertainty and the desirability of knowing the lifetime accurately, I made a direct determination of its lifetime.

Iodine vapor was illuminated by the green line 5461 Å, 1 Å band width, from an A-H4 mercury lamp. This excitation corresponds to the transition $^3\Pi_u(v' = 26) \longleftarrow {}^1\Sigma^+_g(v'' = 0)$. The fluorescence spectra include transitions from v' = 26 to all the ground-state vibrational levels, covering the range 5461 to 9000 Å. The green line was isolated by use of a Wratten filter #62 and neodymium glass; this combination gave 10% transmission at 5461 Å. The fluorescent light passed through a Corning filter #3480 which rejected the green light and gave a 65% transmission at 5795 Å, the principal fluorescent line.

Baker Reagent Analyzed iodine was purified and dried under vacuum (ultimate vacuum of 10^{-5} mm Hg). Iodine was distilled into a Pyrex cell (optical part 1 inch long and 7/8 inch in diameter), which had been baked out at 400°C under vacuum, and was then sealed off. A fluorocarbon grease, Kel F, was used in the stopcocks, since its rate of reaction with iodine is slow. A McLeod gauge was used to read the lowest pressures, but it was separated from the iodine ampoules by a liquid nitrogen trap and wasn't open to the line when the cell was being filled. These precautions were taken to avoid contamination by mercury or other foreign gas, which might conceivably affect the lifetime measurement.

Wood has shown for his particular experimental arrangement that the intensity of fluorescence is linear with vapor pressure when the temperature is below 0°C.[27] These results suggest that self-absorption and collisional deactivation are unimportant below 0°C. Since the amount of self-absorption is dependent on the optical path length, his results are ambiguous to that extent. However, if our optical path lengths are equal to or smaller than Wood's, a measurement at 0°C should yield the true fluorescence lifetime.

By condensing iodine vapor in a side arm of the cell, one could observe the fluorescent signal decrease a factor of six from the room-temperature value. The residual signal was photomultiplier noise.

The results of lifetime measurements at two temperatures (21° and $0^{\circ}C$) are tabulated below.

Lifetime (sec)	$t_{collision}$ (sec)	P_{I_2} (mm Hg)	T ($^{\circ}C$)
4×10^{-7}	6.4×10^{-7}	0.23	21.0
$< 4\times10^{-7}$	4.8×10^{-6}	0.03	0.0

The time between collisions was calculated from the kinetic theory expressions

$$L = 1/\sqrt{2}\,\pi\, n\, \Delta^2,$$

$$v_a = \sqrt{8kT/\pi M},$$

where L is the mean free path and v_a is the average velocity; n is the number of molecules per cc, and the collision diameter Δ was taken as 5.44×10^{-8} cm. Because of the low S/N and the shortness of the lifetime, the accuracy of the measurement is not high. At $21^{\circ}C$ the accuracy is estimated to be of the order of 20%. At $0^{\circ}C$ the uncertainties are larger because both the signal and observed lifetime are smaller. The only significant point about the $0^{\circ}C$ measurement is that its lifetime is smaller than the $21^{\circ}C$ value. The observed lifetime and collision time at $21^{\circ}C$ suggest that collisional deactivation could be just as important as deactivation by fluorescence. If this were the case, the lifetime should increase when the pressure is lowered, since the time between collisions becomes longer. The $0^{\circ}C$ lifetime is shorter, however. The remaining explanation consistent with the data is that self-absorption is more important than collisional deactivation at $21^{\circ}C$. The effect of self-absorption is to increase the observed lifetime. Thus, when the pressure is reduced, both the self-absorption and the lifetime decrease. Admittedly these results don't settle what the true lifetime is, but they do give an upper limit of 4×10^{-7} sec.

Part II

THE PROBABILITY OF SPONTANEOUS NUCLEAR REACTION IN MOLECULAR HYDROGEN

The probability of spontaneous nuclear reaction in molecular hydrogen would appear to be of the same order of magnitude as for two low-energy protons in collision. However, the difference in thickness between a Coulomb and a molecular barrier at the same internuclear distance suggests that the molecule should react more readily. Since the probability of penetrating the barrier is an exponential function of the thickness, small changes in the thickness can result in large changes in the probability. For this reason it seemed worth while to determine the importance of this effect on the over all reaction rate.

The probability per second ("probability current") for reaction[28] can be divided into (a) the probability of finding the two protons in the volume of a deuteron and (b) the probability per sec that they will react once they are inside this nuclear volume. The first probability is given by $\int_I \psi\psi^* dv$, where ψ is the normalized wave function for the two protons, and the integration is over the volume of the deuteron, Region I in Fig. 22. For the sake of simplicity WKB wave functions are used, and thus, the calculation can be expected to be correct to within a few orders of magnitude. If u is defined by $r\psi(r) = u$, the u functions have the general WKB form

$$u = (C_+/\sqrt{g}) \exp\left(\int g dr\right) + (C_-/\sqrt{g}) \exp\left(-\int g dr\right) \quad (9)$$

By restricting the wave function to be finite at the origin, one obtains, from Eq. (9),

$$u_I = \sin \gamma r \qquad (\ell = 0, \text{ S state}),$$

where

$$\gamma = (2\mu/\hbar^2)^{1/2}(E - U_0)^{1/2}.$$

The u functions for Regions II, III, and IV are then found by applying the conditions of continuity in u and du/dr at r = a, and by applying the

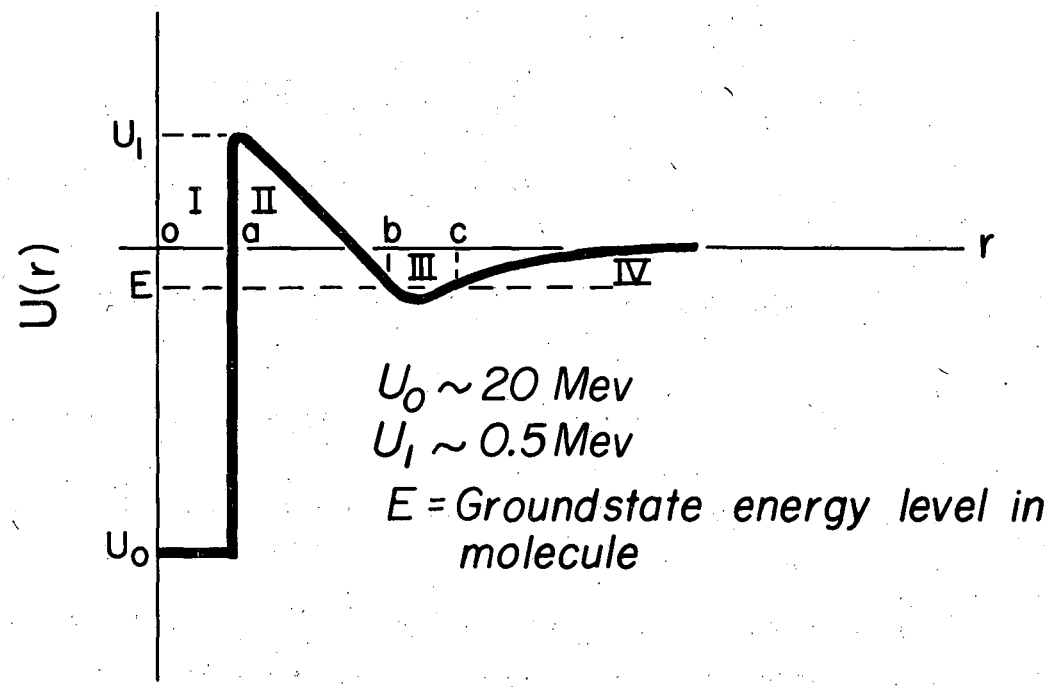

MU-15681

Fig. 22. Potential energy schematic for the hydrogen molecule.
U_0 ~ 20 Mev
U_1 ~ 0.5 Mev
E Ground-state energy level in molecule

connection formulas[29] at b and c. These operations yield

$$u_{II} = C_+ (1/\sqrt{g_{II}}) \exp\left(\int_a^r g_{II} dr\right) + C_- (1/\sqrt{g_{II}}) \exp\left(-\int_a^r g_{II}\, dr\right),$$

$$u_{III} = 2C_+/\sqrt{g_{III}} \left[\exp (G/2)\right] \cos \left[\int_r^c g_{III}\, dr - \pi/4\right] + C_-/\sqrt{g_{II}} \left[\exp(-G/2)\right]$$

$$\cos \left[\int_b^r g_{II}\, dr + \pi/4\right], \tag{10}$$

$$u_{IV} = \left(C_+/\sqrt{g_{IV}}\right)\left[\exp (G/2)\right]\left[\exp\left(-\int_c^r g_{IV}\, dr\right)\right],$$

where $g_{II} = ig_{III} = g_{IV} = \sqrt{(2\mu/\hbar^2)[u(r)-E]}$ and $e^{-G/2} = \exp\left(-\int_a^b g_{II} dr\right)$, the usual penetration factor.

The probability of finding the two protons in the volume of a deuteron is

$$P = (1/N) \int_0^a u_I^2\, dr = \left(a/2 - \frac{1}{4\gamma} \sin 2\gamma a\right) \frac{1}{N}, \tag{11}$$

where N is the normalization and a is the radius of a deuteron. The normalization integral is approximated by $\int_{III} \psi^2_{III}\, dv = \int_{III} u^2_{III} dr$, since the wave function outside Region III is small. In Eq. (10) the second term on the right of u_{III} is negligible since we have $e^{-G/2} << e^{G/2}$, or

$$u_{III} \sim \left[2C_+/(g_{III})^{1/2}\right] e^{G/2} \cos\left(\int_r^c g_{III}\, dr - \pi/4\right). \tag{12}$$

Since the radial part of the ground-state wave function for the molecular nuclei approximates that of a harmonic oscillator, Eq. (12) should approximate a ground-state harmonic-oscillator wave function. This relation can be shown if an average value of g_{III} is taken over the range of integration, i.e., $\overline{g}_{III} = \sqrt{2\mu/\hbar^2\,(E-\overline{U})}$. By the virial theorem we have $\overline{U} = (1/2)E$ for a harmonic oscillator, and $\overline{g}_{III} = (\mu E/\hbar^2)^{1/2}$, where in this case E is measured from the bottom of the potential well. If only the first few terms in the expansion of the cos term in Eq. (12) are compared to the first few terms in the expansion of the harmonic oscillator wave function $\exp\left[-\alpha(r-r_0)^2/2\right]$, it can be seen

that we have

$$\cos\left(\int_r^c g_{III}\,dr - \pi/4\right) \sim \exp\left[-a(r-r_0)^2/2\right],$$

where $a = 4\pi^2\mu\nu/\hbar$. Finally, the normalization can be given with sufficient accuracy by

$$N = \left(4C_+^2/\bar{g}_{III}\right) e^G \int_0^\infty \exp\left[-a(r-r_0)^2\right] dr$$

$$= 2C_+^2 \sqrt{\hbar^2/\mu E}\; e^G \sqrt{\pi/a}\,. \tag{13}$$

Substitution of Eq. (13) into (11) gives the probability for penetrating the molecular barrier,

$$P = \left(\frac{\int_0^a u_I^2\,dr}{2\sqrt{\pi/a}}\right)\left(\frac{\sqrt{\mu E/\hbar^2}}{C_+^2}\right) e^{-G} \tag{14}$$

where

$$C_+ = (\sqrt{g(a)}/2\left[\sin\gamma a + \frac{\gamma}{g(a)}\cos\gamma a\right] \quad \text{and}$$

$$\gamma = \left[\frac{2\mu}{\hbar^2}(E - U_0)\right]^{1/2}.$$

Here $\left(\int_0^a u_I^2\,dr\right)/(2\sqrt{\pi/a})$ is essentially a ratio of a deuteron diameter ($\sim 10^{-13}$ cm) to a molecular internuclear distance ($\sim 10^{-8}$ cm), and $(\sqrt{\mu E/\hbar^2})/(C_+^2)$ is essentially a ratio of the relative velocity of the nuclei in the molecule to the relative velocity of the protons in the deuteron volume, or 10^{-4}. The product of these ratios, $\sim 10^{-9}$, is merely the ratio of the molecular vibrational frequency (10^{14} sec^{-1}) to the oscillation frequency ($\hbar/\mu R^2 = 10^{23}$ sec^{-1}) of the protons in the deuteron volume.

To evaluate the penetration factor e^{-G}, where

$$G = 2\int_a^b \sqrt{\frac{2\mu}{\hbar^2}\left[U(r) - E\right]}\,dr\,, \tag{15}$$

it is necessary to know the potential function U(r) for the molecule. U(r) can be expressed conveniently by the Dunham[30] expansion about the equilibrium internuclear distance r_e, namely

$$U(\xi) = a_0\xi^2 (1 + a_1\xi + a_2\xi^2 + a_3\xi^3 + \ldots) - 31.94 \text{ ev}, \quad * \quad (16)$$

where $\xi = (r-r_e)/r_e$, and the a's are functions of spectroscopic constants,[31] $a_0 = 9.845$ ev, $a_1 = -1.593$, $a_2 = 1.880$, $a_3 = -2.144$, the last three being dimensionless. Equation (16) is quite accurate near the equilibrium distance r_e, but is very inaccurate at small internuclear distances because there are not enough terms to represent the sharply rising repulsive energy of the nuclei. Since it is the shape of the repulsive part of the potential curve that is important in this calculation, Eq. (16) had to be modified. The repulsive energy is simply e^2/r, and if this quantity is subtracted from Eq. (16) to terms in 5th degree in ξ, the remaining energy will be the electron energy. Figure 23 shows a plot of the resulting expression,

$$U_{el} = -51.34 + 19.40\,\xi - 9.55\,\xi^2 + 3.72\,\xi^3 - 0.89\xi^4 - 1.71\xi^5 \text{ ev}, \quad (17)$$

which is seen to be a slowly varying function with distance. At very small distances, however, Eq. (17) gives too small a value, as its intercept is 4 ev smaller than the electron energy of He.

To obtain the behavior of the electron energy at very small internuclear separation, a calculation was made of the energy (considering coulombic interactions only) required to move two protons in a helium atom a small distance apart. The electrons are assumed to have a charge density $e\rho$ which is spherically symmetric and constant in the region of interest. For two protons each at the same distance r from the center of a sphere, the effective negative charge outside is zero, and inside is $e(4/3)\pi r^3 \rho$, and it acts as if it were concentrated at a point at the center of the sphere. The force between the protons and the negative charge is $(2e/r^2)(e(4/3)\pi r^3 \rho)$, and hence the electronic

---

*The energy is considered to be zero when the nuclei are separated from each other, and the electrons from the nuclei and each other, by an infinite distance.

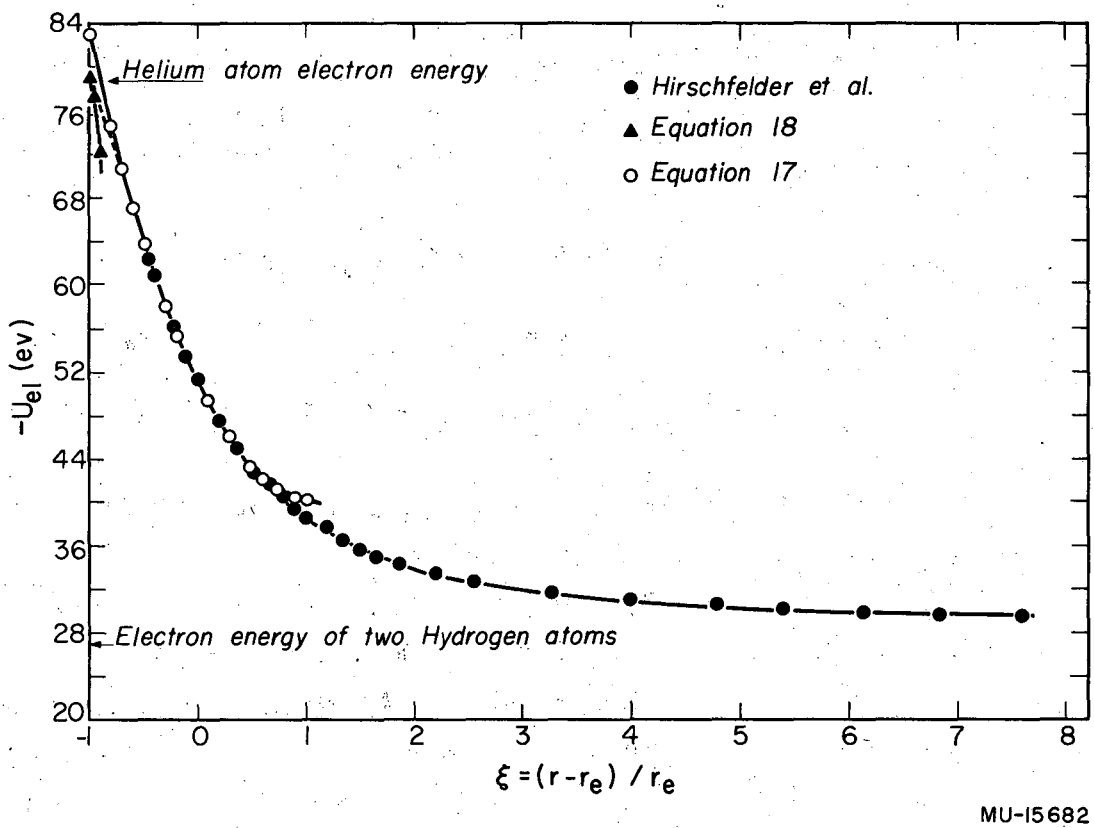

Fig. 23. Electron energy vs internuclear distance in the hydrogen molecule.

energy at very small distances is

$$V = (4/3)\pi e^2 \rho r^2 - 78.98 \text{ ev.} \tag{18}$$

Here ρ was calculated by

$$\rho = \int \psi^2 (2, 1)\, d\tau_1 + \int \psi^2 (2, 1)\, d\tau_2 \tag{19}$$

where the subscripts 1 and 2 refer to the two electrons. Three different wave functions of Kellner and Hylleraas[5] were used in Eq. (19) and they all gave the same limiting behavior. The wave functions used were

$$\psi_I = N_I \exp\left[-1.68\,(r_1 + r_2)/a_0\right],$$

$$\psi_{II} = N_{II} \exp\left[-2\,k\,(r_1 + r_2)/a_0 + 2\,c r_{12}/a_0\right];\quad k = 0.93,\quad c = 0.13;$$

$$\psi_{III} = N_{III}\,\{\exp\left[-z(r_1 + r_2)\right]\}\,(1 + c_1 r_{12});\ z = 1.85/a_0,\quad c_1 = 0.36/a_0.$$

It is seen that a reasonable joining of the plots of Eqs. (17) and (18) can be made at small internuclear distances.

Hirschfelder's tabulation of the potential energy at intermediate and large distances[6] is plotted in Fig. 23 in terms of electron energy, also. His data are the result of a Rydberg-Klein treatment of the vibrational levels and quantum-mechanical calculations at large distances. It is seen that Eqs. (17) and (18) fit on smoothly to his curve and thus extend the data to zero internuclear distance.

The quantity G was determined by adding e^2/r to U_{el} and by integrating Eq. 15 graphically. The probability of penetration, Eq. (14), is given in Table II for the different isotopic reactions,

$$H^1H^1 \longrightarrow H^2 + \beta^+ + \beta^- + \nu \tag{20}$$

$$H^1H^2 \longrightarrow He^3 + \gamma \tag{21}$$

$$H^2H^2 \longrightarrow He^3 + n \tag{22}$$

For comparison the probabilities of penetration were calculated with a Coulombic potential function. For this case G can be evaluated analytically.[34]

The total probability per second for nuclear reaction is the product of the probability for penetrating the barrier and the probability per second for β, γ, or n emission. The probability for beta emission P_β in Eq. (20) is assumed to be completely allowed. Using Salpeter's[35] values for the beta decay constants, one obtains $P_\beta = 1.6 \times 10^{-4}$ sec^{-1}.

The probability for γ emission in Eq. (21) and neutron emission in (22) were taken from Salpeter.[35] The γ-emission value is based on cross-section measurements of thermal neutrons reacting with deuterium ($\Gamma_\gamma = 0.25$ ev), and the neutron-emission value is the result of cross-section measurements of D^2-D^2 reactions at 20 to 250 kev ($\Gamma_n = 5 \times 10^5$ to 10×10^5 ev). The probability for emission is $\Gamma/\hbar$.

A summary of all the data is given in Table II.

Table II

Probabilities (and half life) for barrier penetration (see text).

Molecule	P_{pen}(molecular)	P_{pen}(Coulomb)	$t_{1/2}$ (years)
H^1H^1	2.6×10^{-61}	5.3×10^{-73}	5×10^{56}
H^1H^2	1.1×10^{-69}	3.5×10^{-83}	5×10^{46}
H^2H^2	1.4×10^{-83}	3.5×10^{-100}	1×10^{54}

Column 2 gives the probability of penetration for a molecular barrier, Column 3 the probability of penetration for a Coulomb barrier at the same internuclear distance, and Column 4 the half life, which includes the probability for β, γ, or n emission. The fact that H^1H^2 has the shortest half life appears reasonable, because as the mass increases the probability of penetration decreases but the probability for reaction inside the nuclear volume increases. It is seen that the Coulomb barrier is more difficult to penetrate than the molecular barrier by a factor of about 10^{15}. However, even for the most favorable reaction only one molecule of H^1H^2 in an Avogadro's number would react in 10^{23} years.

ACKNOWLEDGMENTS

I. Special thanks are due Dr. Geoffrey James for his design and construction of the long-lifetime apparatus and for bringing to my attention numerous points associated with lifetime measurements in general. Much of the success of this effort can be attributed to him. In connection with the electronics of the long-lifetime apparatus, I am indebted to Kenneth Lamers for the design and construction.

In addition, I am grateful to Professor William D. Gwinn, Professor Rollie J. Myers Jr., and Harry Robinson for illuminating discussions on the electronic design of the short-lifetime apparatus, to Earl F. Worden for aid in the purification of iodine, and to Mrs. Jane Waite for her secretarial assistance.

Finally, I wish to express my gratitude to Professor Leo Brewer, who directed this research and who is responsible for realizing the potential importance of lifetime measurements in high-temperature chemistry. It is a pleasure to acknowledge his many valuable suggestions during the course of this work.

II. I am indebted to Professor Edward Teller for suggesting Part II of this thesis and for clarifying a number of computational details.

This work was done under the auspices of the U. S Atomic Energy Commission.

Appendix:I The Relation Between Phase Shift and Lifetime

The rate equation for the production of photoactivated molecules X^* is

$$dX^*/dt = k_0 J(t) - kX^*, \qquad \text{(A-1)}$$

where k is the sum of all first-order deactivation constants, including nonradiative processes, and k_0 is determined by the concentration of molecules in the initial level, the optical path length, and the absorption coefficient.

Exciting light J(t) of modulation frequency ω is given by

$$J(t) = (a_0/2) + a\cos \omega t. \qquad \text{(A-2)}$$

Here $a_0/2$ is the average intensity, whereas $(a \cos \omega t)$ is the variation about that average.

Substitution of Eq. (A-2) into (A-1), integration, and use of the definitions

$$\sin \phi = \omega/(k^2 + \omega^2)^{1/2} \text{ and } \cos \phi = k/(k^2 + \omega^2)^{1/2} \qquad \text{(A-3)}$$

yields

$$X^* = (a_0 k_0/2k) + \frac{(k_0 a)^{1/2} \cos (\omega t - \phi)}{(k^2 + \omega^2)^{1/2}} + (ce^{-kt}). \qquad \text{(A-4)}$$

For typical values of $k = 10^{-8}$ sec^{-1}, the exponential term in Eq. (A-4) becomes negligible a fraction of a second after the modulated light is turned on.

The intensity of fluorescent light is given by

$$I = k'X^*, \qquad \text{(A-5)}$$

where k' is the sum of all first-order constants for deactivation by fluorescence. It should be noted that in actual experiment, one observes the variation in the number of photons per second rather than a concentration, since photons are not accumulative. The fluorsecent light follows the kinetics of Eq. (A-4), and thus is out of phase with the exciting light by the angle ϕ. Equation (A-3) shows that the phase angle can be expressed by

$$\tan \phi = \omega \tau = \omega/k,$$

where ϕ is a function only of the modulation frequency ω and the lifetime τ of the molecule in the excited state.

Appendix II: The Effect of Errors in Phase Angle on the Lifetime

The phase angle ϕ and lifetime τ are related by

$$\tan \phi = \omega\tau. \tag{A-6}$$

Equation (A-6) in differential form is

$$d \tan \phi = \omega d\tau \tag{A-7}$$

and dividing Eq. (A-7) by (A-6) yields

$$d\phi/\sin\phi \cos\phi = d\tau/\tau. \tag{A-8}$$

Thus, the fractional error in lifetime is largest when the phase angle is near 0 or $\pi/2$. Obviously, at $\phi = \pi/4$ the errors in ϕ reflect a minimum error in the lifetime.

REFERENCES

Part One

1. R. S. Mulliken and C. Riehe, Repts. Progr. in Phys. 8, 231 (1941).
2. Peter Pringsheim, Fluorescence and Phosphorescence (Interscience, New York, 1949), p. 250.
3. William T. Hicks, Spectroscopy of High-Temperature Systems (thesis), UCRL-3696, Feb. 1957, p. 62-66.
4. J. White, J. Chem. Phys. 8, 79, 459 (1940).
5. O. Oldenberg and F. Rieke, J. Chem. Phys. 6, 439, 779 (1938).
6. P. J. Dyne, J. Chem. Phys. 28, 999 (1958).
7. A. C. G. Mitchell and M. W. Zemansky, Resonance Radiation and Excited Atoms (Cambridge University Press, London, 1934), p. 100; p. 201, 229 et seq., and 331.
8. Private communication from Leo Brewer, UCRL.
9. L. A. Tumerman, J. Phys. (U.S.S.R.) 4 151 (1941).
10. Ernest A. Bailey, Jr., Lifetimes of Fluorescent Substances, (thesis), University of California, June 1952; E. A. Bailey and G. K. Rollefson, J. Chem. Phys. 21, 1315 (1953).
11. Paul R. Kromann, The Effect of Environment on Lifetimes of Fluorescent Substances (thesis), University of California, June 1957.
12. D. R. Stull and G. C. Sinke, Thermodynamic Properties of the Elements (American Chemical Society, Washington, D. C., 1956) p. 188.
13. P. Debye and F. W. Sears, Proc. Natl. Acad. Sci, U.S. 18, 409 (1932).
14. P. Biquard and R. Lucas, J. Phys. radium 3, 464 (1932).
15. W. G. Cady, Piezoelectricity (McGraw-Hill, New York, 1946).
16. Britton Chance et al., Waveforms (McGraw-Hill, New York, 1949), p. 138.
17. Du Mont Multiplier Photo-tubes, Descriptions and Specifications, 1955.

18. Frederick A. Kirsten, Results of Transit-Time Measurements on Three C 7187A Photomultiplier Tubes, University of California Radiation Laboratory Report No. UCID-19, Dec. 1955; Questin A. Kerns and Frederick A. Kirsten, Results of Tests on Two C 7232 Experimental 16-Stage Multiplier Phototubes, UCID-97, Nov. 1956.
19. Earl F. Worden, (thesis), University of California, Feb. 1959 (?).
20. Gerhard Herzberg, Molecular Spectra and Molecular Structure I (Van Nostrand, New Jersey, 1957), p. 382.
21. R. W. Wood, Physical Optics (Macmillan, New York, 1934), p. 623 et seq.
22. A. F. Trotman-Dickenson, Gas Kinetics (Academic Press, New York, 1955), p. 82 et. seq.
23. F. Rossler, Z. Physik 96, 251 (1935).
24. W. C. Wood and E. Rabinowitch, J. Chem. Phys. 4, 358 (1936).
25. J. C. Polanyi, Can. J. Chem. 36, 121 (1958).
26. C. Arnot and C. A. McDowell, Can. J. Chem. 36, 114 (1958).
27. R. W. Wood, Phil. Mag. 27, 531 (1914).

Part Two

28. H. Bethe, Phys. Rev. 55, 434 (1939).
29. David Bohm, Quantum Theory (Prentice-Hall, New York, 1952), p. 273.
30. J. Dunham, Phys. Rev. 41, 721 (1932) or A. G. Gaydon, Dissociation Energies (Chapman and Hall, London, 1953), p. 32.
31. B. Rosen, Données Spectroscopiques Concernant Les Molecules Diatomiques (Hermann, Paris, 1951).
32. L. Pauling and E. Wilson, Introduction to Quantum Mechanics (McGraw-Hill, New York, 1935), p. 224.
33. Hirschfelder, Curtiss, Bird, Molecular Theory of Gases and Liquids (Wiley, New York, 1954), p. 1060.

34. G. Gamov and L. Critchfield, Theory of Atomic Nucleus and Nuclear Energy-Sources (Clarendon, Oxford, 1949), p. 173.

35. E. Salpeter, Phys. Rev. 88, 547 (1952); 97, 237 (1955).